Gasification of woody biomass in a novel indirectly heated bubbling fluidized bed steam reformer

Tsekos, C.; del Grosso, M.; de Jong, W.

DOI
10.1016/j.fuproc.2021.107003

Publication date
2021

Document Version
Final published version

Published in
Fuel Processing Technology

Fuel Processing Technology 224 (2021) 107003

Contents lists available at ScienceDirect

Fuel Processing Technology

journal homepage: www.elsevier.com/locate/fuproc

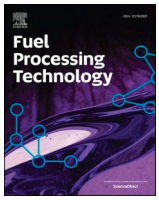

Research article

Gasification of woody biomass in a novel indirectly heated bubbling fluidized bed steam reformer

C. Tsekos [a,*,1], M. del Grosso [a,1], W. de Jong [a,b]

[a] Faculty of Mechanical, Maritime and Materials Engineering, Process and Energy Department, Delft University of Technology, Leeghwaterstraat 39, Delft 2628, CB, Netherlands

[b] Faculty of Science and Engineering Chemical Technology, Engineering and Technology Institute of Groningen, Nijenborgh 4, 9747, AG, Groningen, the Netherlands

ARTICLE INFO

Keywords:
Allothermal gasification
Biomass
Steam reforming
Synthesis gas

ABSTRACT

Within this work, a novel 50 kW_{th} indirectly heated bubbling fluidized bed steam reformer (IHBFBSR) is presented, along with its commissioning experiments. In the IHBFBSR, heat is provided through two radiant tube natural gas burners in the bed and the freeboard area. The aim of this innovative design is sufficient heat provision for biomass steam reforming and cracking reactions and heat loss reduction, thus allowing the possibility of scaling-up to an industrial level. Experiments were performed with two woody biomass feedstocks and two bed material particle sizes under different operating conditions (steam to biomass ratio, lambda, temperature), in order to identify the setup's main characteristics. Product gas composition and quality, as well as the cold gas efficiency of the IHBFBSR were in reasonable agreement to similar systems, however carbon conversion prediction needs further improvement. H_2 production and tar removal are favoured by small bed material particle sizes as well as by char accumulation in the bed area. Furthermore, air injection above the bed led to improved H_2/CO ratios and lower tar yields compared to when air is used as a fluidization agent. Overall, it was shown that the IHBFBSR technology constitutes a promising development in the field of biomass allothermal gasification.

1. Introduction

Sustainable resources for heat and power generation as well as for fuels and chemicals production have been attracting a lot of interest amidst concern for environmental change, the depletion of fossil fuel reserves, as well as the increasing need for energy self-reliance. Biomass, the third most abundant fuel resource after coal and oil, constitutes such a potentially clean and renewable fuel, which is also readily available worldwide. Biomass thermochemical conversion processes constitute interesting options for the abovementioned products, with pyrolysis, torrefaction, gasification, combustion and hydrothermal liquefaction comprising the main employed thermochemical conversion methods [1]. Gasification in particular, is the thermochemical conversion process by which carbonaceous materials are converted to a fuel gas or a chemical feedstock in a reducing (oxygen deficient) environment requiring heat [2].

One type of gasifier's classification is based on the gas-solid interaction within the unit and it includes fixed or moving bed (downdraft, updraft, crossdraft) gasifiers, fluidized bed gasifiers (bubbling, circulating and dual) and entrained flow gasifiers (top-fed and side-fed). Another possible way to classify a gasifier is by the gasifying medium employed (air, CO_2, steam, etc.) [2,3]. An important distinction between gasifier types, can also be made according to the way that the heat required for the gasification of a feedstock is provided to the system. Autothermal or direct gasification occurs when the feedstock is partially oxidized by the gasification agent (usually air or O_2). This way, the heat required for the fuel heating, drying, pyrolysis and gasification reactions is provided by exothermal oxidation reactions within the gasifier. When an oxidizing agent is not employed, an external energy source is required and the process is then called allothermal or indirect gasification. Steam is most commonly used as an allothermal gasification agent [4,5]. In regards to autothermal gasification, the biggest limitation lies within the separation/removal of diluent gases such as N_2, either downstream (from the syngas) or upstream (from air) the gasification unit [6]. Thus, allothermal gasification technologies constitute an attractive option.

According to Karl and Pröll [7], the heat required for the operation of allothermal gasifiers can be provided either by the discontinuous

* Corresponding author.
E-mail address: C.Tsekos@tudelft.nl (C. Tsekos).
[1] Equal contribution.

https://doi.org/10.1016/j.fuproc.2021.107003
Received 1 July 2021; Received in revised form 27 August 2021; Accepted 28 August 2021
Available online 3 September 2021

intermittent operation of a single fluidized bed, or by the circulation of particles between two interconnected fluidized beds, or through heat transfer surfaces. The first category regards mainly Winkler's fluidized bed gasifier (1922), where heating of the fluidized bed was performed through air (or later O_2) blown combustion up to 1100–1200 °C, repeatedly followed by steam blown gasification. The latter two technologies have seen much more application and development in the recent years. The interconnected fluidized beds gasification technology, or as it is most commonly referred to: Dual Fluidized Bed (DFB) gasification, includes the utilization of two separate gasification and combustion reactors [8,9]. Several large scale applications of the DFB technology have been presented in the recent years including an 8 MW_{th} demonstration plant in Güssing (Austria, 2002), a 8.5 MW_{th} plant in Oberwart (Austria, 2008), a 15 MW_{th} plant in Senden, Germany [10] and the Gothenburg Biomass Gasification (GoBiGas) 32 MW_{th} plant, along with the supporting 2–4 MW research gasifier at the Chalmers University of Technology, Sweden (2005 and 2007, respectively) [11]. It should also be mentioned that two demonstration plants in Nongbua, Thailand (1 MW_{th}) and Daigo, Japan (1.4 MW_{th}) [12], as well as an upcoming project (2023) Gaya, France [13] are inspired by the Güssing gasifier. In general, all the aforementioned plants employ the DFB "Güssing concept", as it was referred to and described in [7]. Other notable DFB gasification systems are Battelle's FERCO gasification process, also referred to as SilvaGas or Taylor gasification process (40 MW_{th}, Burlington – Vermont, USA) [14] and the 30 kW MILENA gasifier of TNO (Netherlands), which is still in operation [15–17]. More DFB gasification systems along with important technical details are presented by Karl and Pröll in [7] and more recently by Larrson et al. in [18] and Hanchate et al. in [19].

Heat exchanger configurations for the delivery of the heat required for the operation of a gasifier can be designed in different ways. In one concept, the gasification area is completely separated from the "heat provision reactor" and therefore a plethora of different fuels and/or processes for heat supply can be employed. Such a reactor was proposed for the first time by Juentgen and van Heek in 1975 [20], employing helium produced from nuclear reactors at high temperatures (HTR). According to Karl [21], the large number of heat exchangers required, due to poor heat transfer between the heat carrier gas and the inner tube surface of the heat exchangers, hindered the progress of this project. The concept was revisited in the following decades in an effort to reduce the gasification temperature, in order to minimize the effect of poor heat transfer, through the application of different catalyst types and configurations [22–24], however no commercial demonstrations have been presented so far. In the early 90s the MTCI technology was employed in a pilot scale black liquor gasifier in Erode, India and in several pulp mills in North America in similar configurations [25,26]. The MTCI gasifier is a steam blown atmospheric fluidized bed reactor, employing in-bed heat exchanger tubes for heat provision. Part of the gas produced from gasification was burned in a pulse combustor that fed the heat exchanger tubes. The highly turbulent flue gas and the low frequent acoustic oscillations produced from pulse combustion can achieve improved heat transfer rates compared to conventional heat exchangers [7,26]. The most recent concept in indirectly heated fluidized bed gasifiers is the Biomass Heatpipe Reformer (HPR), which was presented for the first time in 2001 and has been commercially developed by Agnion Inc. with a 500 kW demonstration plant in Pfaffenhofen, Germany and two commercial 1 MW plants in Grassau, Germany and Auer, Italy. The plant in Grassau was not a success due to very high tar levels, creep behaviour of the heat pipes and reduced cold gas efficiencies due to the combustion chamber design [27]. In 2015, an advanced Heatpipe Reformer pilot plant of 100 kW with optimized combustor design was commissioned in Erlangen-Nuremberg [28]. According to this concept, gasification takes place in a pressurized chamber and the heat is provided by a combustion chamber which is located below it, through a number of heat pipes. It should be mentioned, that both the gasifier and the combustor are fluidized reactors. The two fluidized beds are connected via a series of heat pipes, where the working fluid (usually an alkali metal such as Na, K, etc.) evaporates on one side (combustor) and condenses on the other (gasifier) [28–30]. The use of the Heatpipe concept (evaporation-condensation) is claimed to lead to high heat transfer coefficients and smaller heat transfer areas by a factor of 10 to 20 [21].

In this work, a novel indirectly heated biomass gasification concept is presented along with the respective commissioning experiments. In particular, an atmospheric pressure 50 kW_{th} indirectly heated bubbling fluidized bed steam reformer (IHBFBSR) was designed, built and commissioned by the Dutch company Petrogas - Gas Systems in collaboration with the Process and Energy Department of the Delft University of Technology. The novelty of the reactor lies within the method of heat provision for the gasification reactions. For this purpose, two radiant tube natural gas burners, one in the bottom (bed area) and one in the top (freeboard) of the reactor, are employed (Fig. 1). Its design aims at the reduction of heat losses, the provision of enough heat for the realization of the biomass steam reforming and cracking reactions and the exploration of scale-up possibilities to an industrial scale process. The commissioning experiments presented in this work are aimed at obtaining understanding of the operation characteristics, fuel conversion and raw product gas composition.

2. The Indirectly Heated Bubbling Fluidized Bed Steam Reformer (IHBFBSR)

In this section, the novel 50 kW_{th} Indirectly Heated Bubbling Fluidized Bed Steam Reformer (hereby referred to as IHBFBSR) is presented. A simplified process flow chart of the reactor is presented in Fig. 2. In this reactor, combustion and gasification reactions are separated to a

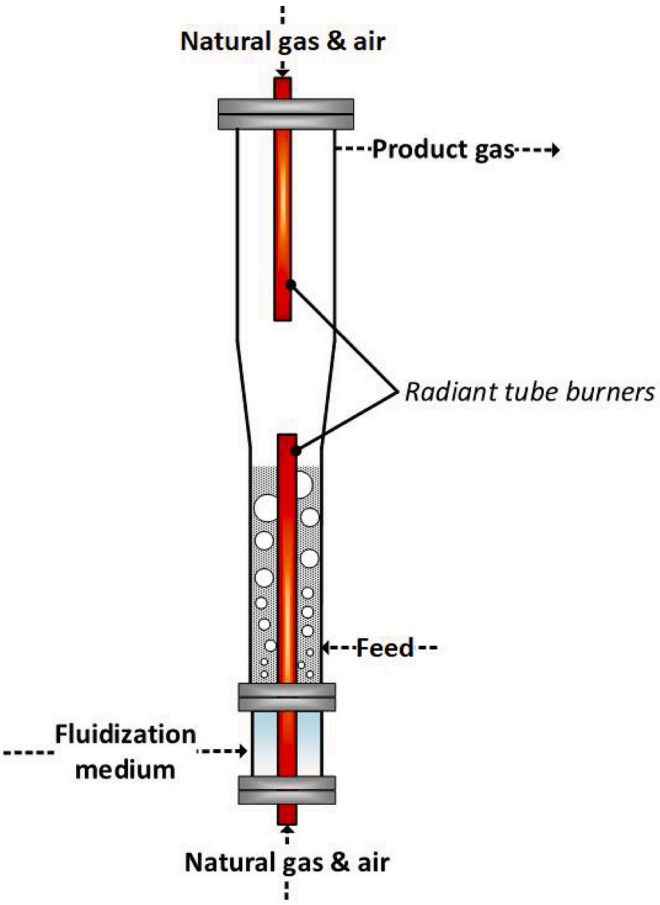

Fig. 1. Conceptual design of the indirectly heated bubbling fluidized bed steam reformer (IHBFBSR).

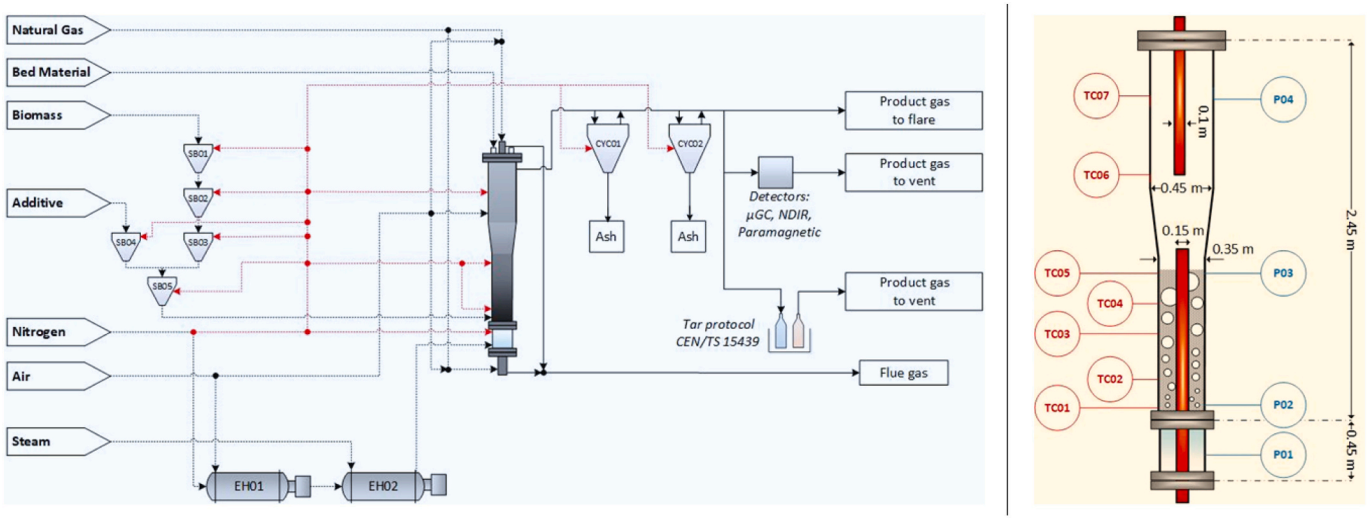

Fig. 2. IHBFBSR simplified process flow chart (left)/ Basic dimensions and main sensors location in the IHBFBSR reactor chamber. P: pressure gauge, TC: thermocouple (right).

great extent in a novel way, thus avoiding the dilution of the product gas.

The gases that can be employed as fluidization agents in the IHBFBSR are N_2, air and steam. Steam is produced at a working pressure between 3.5 and 5 bar and then expanded to near atmospheric conditions, depending on the supply. Air and/or nitrogen, which is mainly used during warming up, pass initially through a 4.5 kW preheater (EH01), where they are heated up to 150 °C. The steam, along with the gases that are preheated by EH01, are fed to a second 6 kW preheater (EH02). The gasification media are all fed to the reactor at about 200 mbarg typically. Air can also be directly fed into the freeboard as a measure for tar destruction. The secondary air injection point is located ~90 cm below TC06 (Fig. 2). The radiant tube burners are supplied with air and natural gas at 80 mbar and 60 mbar, respectively. N_2 is also distributed to the pressure gauges in the reactor (Fig. 2) (5 ml/min each) and the two cyclones, as well as to the biomass and additive bunkers (4 kg/h).

The reactor is manufactured out of 310S (AISI) steel with a wall thickness of 4.78 mm and a height of roughly 3 m. It is insulated with a 200 mm three layer matrass. Gases are fed in the windbox and subsequently in the reactor, through a distributor plate consisting of 50 tuyeres each with two 2 mm holes drilled in a 25° angle (downwards). As presented in Fig. 2, the temperature in the reactor is monitored by thermocouples located in and above the bed zone. The last thermocouple (TC07) is located at almost the same height as the product gas outlet which is on the reactor inner wall. Pressure gauges are located in four spots within the IHBFBSR along with differential pressure transmitters, that allow the recording of the pressure drop over the distributor plate, the bed zone and the freeboard. In general, data from the various instruments are recorded through a SCADA/PLC coupling employing a LabVIEW interface. The system obtains and records data every 10 s.

The two self-recuperative ceramic burners utilized for gasification heat provision were supplied by WS – Wärmeprozesstechnik GmbH. Both of them are placed inside metal radiant tubes in order to protect the ceramic burners from the bed material blasting. Both burners operate in an on/off mode; the bottom burner is controlled by the average values of thermocouples TC01 – TC05 and the top burner by thermocouple TC07. For both burners the maximum allowable set point was at 850 °C according to the safety regulations. The burners operate at a constant capacity of 20 kW_{th} and 12 kW_{th} for the bottom (REKUMAT C100) and top one (REKUMAT C80), respectively. Regarding the bottom radiant tube, its total main body length is ~1.7 m and 1.2 m of this is situated in the bed area. The bottom part of the radiant tube heats up the windbox, as shown in Fig. 2. The top radiant tube is smaller than the bottom one, both in terms of diameter (0.1 m versus 0.15 m) and of total main body length (1.3 m versus 1.7 m).

Part of the product gas, after the cyclones, is led to the gas analysis section. The gas analysis line is traced at 400 °C and a heated candle filter (350 °C) is used as the main method of char and ash particles removal. After this point, part of the gas is channelled to the tar sampling system, where tars are sampled according to the Tar Protocol CEN/TS 15439 [31]. Downstream the tar protocol are placed, a pump a flowmeter and a gas meter. The rest of the gas passes through a water cooled condenser and is led to the gas analysis section. There four bottles, three of them filled with isopropanol and one filled with silica gel, are used for tar and moisture removal. Subsequently a Whatman 55 mm paper filter and the pump follow and from there the gas is led to the detectors. A micro-GC, samples from the product gas stream every 4 min, measuring CO, CO_2, H_2, CH_4 and N_2. Then the gas flow splits into two streams each passing though the O_2 detector and the Non-Dispersive Infrared Detector (NDIR), for the measurement of CO and CO_2. The use of these analysers is necessary for the online monitoring of the experiment.

3. Materials and methods

3.1. Feedstocks, bed material and analytical equipment

The biomass feedstocks employed in this work were two different types of A-quality residual wood (termed Premium Green and Excellent Red), supplied by the company Labee Group Moerdijk B·V, the Netherlands. Both feedstocks were supplied in the form of pellets with a length of 2 cm and a diameter of 0.6 cm. Premium Green (PG), consists of woodchips, sawdust and wood shavings of brown leafage wood from Dutch secondary forest biomass. Excellent Red (ExR), is derived from white pine wood woodchips, originating from Scandinavian countries and Russia. Table 1 shows the proximate and ultimate analysis of the two feedstocks. The moisture and ash content of the biomass species was determined according to the NREL/TP-510-42621 [32] and NREL/TP-510-42622 [33]. Fixed carbon and volatile content for each feedstock were determined with an SDT Q600 Thermogravimetric Analyser (TGA). In this analysis, ~3 mg of sample were heated at 10 °C/min in an inert atmosphere (100 ml/min of N_2) up to 600 °C and held there for 10 min. Afterwards, at the same temperature, combustion with 100 ml/min

Table 1
Proximate analysis, ultimate analysis and Lower heating Value (LHV) for the two woody biomass feedstocks (PG and ExR) employed in the IHBFBSR commissioning experiments.

	Proximate analysis				Ultimate analysis					LHV (MJ/kg)
	Moisture (% wt)	Volatiles (% wt d.b.)	Fixed carbon (% wt d.b.)	Ash (% wt d.b.)	C (% wt d.b.)	H (% wt d.b.)	N (% wt d.b.)	S (% wt d.b.)	O (% wt d.b.)	
PG	5.08	78.13	21.15	0.73	48.41	6.02	0.3	0.01	44.53	18.98
ExR	5.57	84.07	15.44	0.49	47.88	6.44	0.06	0.01	45.13	19.5

of air was performed for 10 min. The ultimate analysis was performed using a Vario MICRO CHNS analyser and the lower heating value (LHV)[2] of the two fuels was determined using a Parr 6772 Calorimetric Thermometer.

Corundum, which is an aluminium oxide (Al_2O_3) containing also traces of iron oxide, titanium oxide and silica, was used as the bed material for the IHBFBSR commissioning experiments. This material, supplied by Unicorn ICS B.V., has a density of 3940 kg/m^3, a hardness of 9 Mohs and its melting point is 1950 °C. The weighted average particle diameter for the bed material employed in the experiments was 590 μm (F046) and 490 μm (F054), which classifies them in the Geldart B category (sand-like) of solids in bubbling fluidized beds [34]. It has a very high hardness, thus the probability of fines production due to attrition of the particles is reduced. Furthermore, depending on the fluidization conditions, it has very good heat distribution properties [35].

The analysis of the permanent gases (CO, CO_2, CH_4, H_2 and N_2), was performed using a Varian CP4900 micro-Gas Chromatograph. Separation of the individual gases was achieved on a 1 m CP-COX column and detection/quantification by a TCD detector using Argon as carrier gas. For O_2, a Hartmann & Braun Magnos 6G paramagnetic detector was applied, while for CO and CO_2, a Hartmann & Braun Uras 10 NDIR was used. For tar detection and quantification, an Agilent Technologies 7890A GC-FID system was employed. The acquisition run time was 90 min, including an increase of temperature of the oven from 50 to 300 °C at 5 °C/min rate and a hold time of 38 min. The species measured were: benzene, toluene, ethyl benzene, naphthalene, acenaphthylene, fluorene, anthracene, phenanthrene, pyrene, chrysene, benzo(*a*)anthracene, benzo(*k*)fluoranthene, benzo(*a*)pyrene, dibenz(*a,h*)anthracene, indeno (1,2,3-*cd*)pyrene, benzo(*b*)fluoranthene. Moisture content was determined using a Mettler Toledo V10S volumetric Karl Fischer Titrator with a polarized DM143-SC sensor.

3.2. Definition of main process parameters

The experiments conducted, apart from varying biomass type and bed material particle sizes, also explored different operational conditions. In particular, steam gasification experiments were conducted with different steam to biomass ratios (STBR) and different λ. These two parameters are described according to the following formulas:

$$STBR = \frac{\dot{m}_{steam} + X_{H_2O} \bullet \dot{m}_{biomass}}{\dot{m}_{biomass\ (d.a.f.)}} \quad (1)$$

$$\lambda = \frac{\dot{m}_{O_2} / \dot{m}_{biomass\ (d.a.f.)}}{\left(\dot{m}_{O_2} / \dot{m}_{biomass\ (d.a.f.)}\right)_{stoichiometric}} \quad (2)$$

Where, $\dot{m}_{steam}$ is the steam mass flow rate, $\dot{m}_{biomass}$ the biomass feedstock mass flow rate and $\dot{m}_{O_2}$ is the oxygen mass flow rate. In the IHBFBSR, oxygen is supplied by air. STBR correlates the total amount of steam provided either directly as a feed or as biomass moisture, to the dry-ash-free biomass input. Lambda (λ), or stoichiometric oxygen ratio is usually employed for identifying different oxidation regimes. Typically, λ ranges between 0.2 and 0.4, while the STBR varies between 0.5 and 2 [35]. In regards to the output parameters which were used in order to evaluate the experiments conducted, emphasis was put on the cold gas efficiency (CGE), carbon conversion efficiency (CCE), permanent gas composition and tar and content [36]. The definitions of the calculated process parameters is given below, adapted from [37]. In addition the overall efficiency (OE) of the process was calculated based on a simple energy balance as shown also below.

$$CGE = \frac{\dot{m}_{product\ gas} \bullet LHV_{product\ gas}}{\dot{m}_{biomass} \bullet LHV_{biomass}} \quad (3)$$

$$OE = \frac{\dot{m}_{product\ gas} \bullet LHV_{product\ gas}}{\dot{m}_{biomass} \bullet LHV_{biomass} + \dot{Q}_{Burners} + \dot{Q}_{Preheaters}} \quad (4)$$

$$CCE = 1 - \frac{\dot{m}_{C,residue}}{\dot{m}_{C,biomass}} \quad (5)$$

3.3. Experimental procedure and overview

Before each test, 75 kg of bed material (corundum F046 or F054) was loaded in the reactor. This amount of bed material corresponds to a stationary bed height of roughly 0.59 m. Each experiment was initialized by warming up the reactor to an average bed temperature of 850 °C. The average bed temperature was defined as the average values of thermocouples TC01 – TC05. This process included two separate steps. The first step started by introducing the maximum fluidization media flow, which corresponds to 30 kg/h of N_2 and 22 kg/h of air. At the same time, both burners were turned on with a set point of 850 °C, along with the two preheaters. In order to reach the designated temperature the heat provided by the radiant tube burners does not suffice. Therefore a biomass combustion step was added to the warming up process. This step of the warming up process, was performed with 22 kg/h of air and the appropriate amount of biomass feedstock in order to achieve stoichiometric combustion. The biomass flow rate for stoichiometric combustion is approximately 4 kg/h for both PG and ExR, since the two species have similar compositions. It should also be mentioned, that preliminary combustion tests were performed with both biomass species, under the exact same conditions as the ones employed for the aforementioned warming up step. These tests showed that close to full conversion was achieved during this process, since no char was found in the bed (particle or fine form) or in the cyclones. Furthermore, after the completion of the combustion warming up step, the cyclones were emptied from the combustion produced ashes, in order to avoid interference with the subsequent measurements in the gasification phase.

After this point the O_2 and NDIR detectors which are measuring gas composition online, as well as the micro-GC were started. When the set point for the bottom burner was reached gasification could be initiated. Steam and air were supplied to the system according to the STBR and λ required. The goal was to achieve steady state gasification operation, which corresponds to relatively stable temperature and gas composition profiles. When steady state was achieved, tar sampling using the tar protocol was initiated. According to this protocol, tar sampling should

[2] The lower heating value of a fuel is defined as the amount of heat released by the combustion of a specified quantity of it, minus the heat of vaporization of the water produced [2].

be performed for at least 30 min with a gas flow rate between 0.1 and 0.6 Nm^3/h. During the steady state, the average value of each gas as measured from the micro-GC, was used for the derivation of the gas composition, which is presented in this work. As it will be thoroughly presented in the results and discussion section, the employment of different lambda values (λ) between the various experiments, influences also the operational temperatures throughout the system. This differentiation occurs due to the varying degree of char and/or biomass oxidation reactions that take place when different lambda values are employed. The reduction of the extent of oxidation reactions in the case of low λ (and therefore low temperature) experiments led to increased char accumulation in the bed. That was evident by the increased bed height as observed through the thermocouple values.

During cooling down, in order to preserve the char in the reactor for weighing and future analysis, only N_2 was fed in the reactor at its maximum flow rate. The tar samples obtained were collected in bottles and refrigerated at ~5 °C. Two samples of each tar protocol were taken in HPLC vials for the subsequent tar analysis (GC-FID) and Karl Fischer titration. After cooling down, the bed material was collected and subsequently sieved to separate the bed material from the larger char particles. This was achieved with the use of a 500 or 600 μm sieve, depending on the bed material used, in combination with a Retsch AS300 sieve shaker. The char was weighed and stored, while the bed material was also weighed and five samples from it were combusted with air at 600 °C for 4 h in a muffle furnace (Nabetherm 30), until constant weight (±0.3 mg). The difference in weight was assumed to correspond to the amount of fine char particles. The combustion process was also performed for the material removed from the cyclones, which contained both ashes and char particles. Through these three processes, the char yield and therefore also the ash yield, of each experiment was determined.

3.4. Experimental matrix

Table 2 presents the experiments performed within this work. For the cases with two set points, the first one corresponds to a time before the final steady state was established. The average bed temperature (Average bed T), corresponds to the thermocouples TC01 to TC03 average, since for every experiment the bed area always included only these thermocouples. The experimental results are discussed in Section 4.

Experiments were conducted with two sizes of bed material (F054 and F046), as well as with two different kinds of wood residue feedstocks. Furthermore, for each bed and biomass specie, STBR values of 0.8, 1 and 1.2 were employed as well as different lambdas (λ) which also led to different bed temperatures. According to the values of λ employed, the overall temperature of the gasifier is influenced. The temperature profiles throughout the system for various operational conditions are presented in Appendix A (Figs. A.1 and A.2). Experiments with an average bed temperature above 800 °C will be hereby referred to as high temperature (HT) experiments, while experiments with lower average bed temperatures will be referred to as low temperature (LT) experiments. Additionally, it should be mentioned, that in the case of HT experiments with ExR, the average bed temperature dropped significantly during the initiation of steam/air gasification when a λ of 0.2 was employed. To maintain a bed temperature comparable to the PG experiments λ was increased to 0.23. In order to explain this difference noted between the two biomass feedstocks one can look at their compositional characteristics (Table 1). Despite the fact that the LHV values are slightly higher for PG (19 MJ/kg versus 19.5 MJ/kg), the difference between the values is too small. On the contrary, the much lower fixed carbon content of ExR (15 wt% versus 21 wt%), can presumably lead to less char formation, mainly from the initial pyrolysis stage of the gasification process. The subsequent char oxidation is assumed to be the main reason for maintaining the desired gasification temperature, since the LHV of biomass char is in general much higher compared to the parent biomass [2]. Therefore, the reason for the observed difference in maintaining the required process temperature between the two feedstocks, can be attributed to the lower fixed carbon content of ExR.

Apart from the aforementioned parameters, the effect of the injection of *sec*ondary air in the freeboard (abbreviated as sec. air in Table 2) and the duration of the experiment were also studied. Secondary air injection will be investigated in terms of its efficiency as a tar reduction method, due to the introduction of oxidizer (O_2) and the local increase of temperature. Tar reduction efficiency will be compared to the effect on the product gas composition. This method was employed, due to the presence of the burner in the freeboard. Depending on the effectiveness of the method, the exothermicity of the oxidation reactions can lead to potential energy savings for the top burner. Furthermore, the straightforward and simple implementation of this concept in the IHBFBSR, was an advantage for the commissioning phase of the associated project. The duration of the experiment, as briefly mentioned before, can be linked to the accumulation of char in the bed area for LT experiments. Therefore,

Table 2
Experimental matrix for the PG and ExR steam gasification experiments conducted in the IHBFBSR.

#	Set point	Bed Material	Biomass	Average bed T-°C	Steam-kg/h	Biomass-kg/h	Air-kg/h	Sec. air- kg/h	λ	STBR
1	–	F054	PG	839 (± 1)	9.0	10	11.3	0	0.20	1.0
2	–	F054	PG	840 (± 1)	10.8	10	11.3	0	0.20	1.2
3	–	F054	PG	836 (± 1)	7.3	10	11.2	0	0.20	0.8
4	–	F046	PG	833 (± 1)	10.4	10	11.3	0	0.20	1.2
5	SP1	F046	PG	831 (± 1)	7.3	10	11.3	0	0.20	0.8
	SP2	F046	PG	832 (± 1)	7.3	10	11.3	0	0.20	0.8
6	SP1	F054	ExR	826 (± 6)	10.5	10	13.3	0	0.23	1.2
	SP2	F054	ExR	839 (± 1)	10.7	10	11.3	0	0.20	1.2
7	SP1	F046	ExR	816 (± 6)	10.6	10	13.3	0	0.23	1.2
	SP2	F046	ExR	833 (± 1)	10.5	10	11.3	0	0.20	1.2
8	SP1	F046	ExR	740 (± 14)	8.8	8	1.9	0	0.04	1.2
	SP2	F046	ExR	711 (± 1)	8.7	8	1.9	0	0.04	1.2
9	SP1	F046	ExR	733 (± 12)	8.6	8	1.9	8	0.04	1.2
	SP2	F046	ExR	704 (± 1)	8.7	8	1.9	8	0.04	1.2
10	SP1	F046	ExR	724 (± 8)	8.8	10	1.9	4	0.03	1.0
	SP2	F046	ExR	702 (± 3)	8.8	8	1.9	4	0.04	1.2
	SP3	F046	ExR	710 (± 1)	8.7	8	1.9	4	0.04	1.2
11	SP1	F054	ExR	717 (± 10)	8.7	8	1.9	4	0.04	1.2
	SP2	F054	ExR	715 (± 1)	8.7	8	1.9	4	0.04	1.2
12	SP1	F054	ExR	727 (± 9)	8.9	8	1.9	8	0.04	1.2
	SP2	F054	ExR	722 (± 1)	8.8	8	1.9	8	0.04	1.2

an early tar sampling (SP1) was performed in order to be able to compare the two states of the experiment. This is mainly in terms of the effect of char's presence on the product gas' tar content and overall composition.

4. Experimental results and discussion

4.1. Effect of STBR and bed material particle size

In this section, the effect of STBR and the bed material particle size is examined, using the experiments 1, 2, 3, 4 and 5 (SP2) conducted with PG (Table 2). These experiments were performed in the same bed temperature range (833–840 °C) and at λ = 0.2. In terms of the temperature profile developed in the reactor, the average values during the steady state for the TC04 – TC05 region were higher by 11 °C, on average, for the experiments conducted with F046 compared to F054. This is, however, compensated by the reverse behaviour for the TC01 – TC03 area of the bed, leading to an average TC01–05 temperature of 850 °C for all the experiments. The difference lies mostly in the fluidization and thus heat transfer characteristics of the two bed material sizes. In general, it is observed that the smaller bed material size (F054) leads to a lower temperature difference between the bed area and the area directly above it, hinting possibly to improved heat transfer compared to the larger bed material size (F046). Regarding the freeboard area (TC06 and TC07), the temperatures were the same for all the experiments conducted (864 °C and 849 °C respectively).

4.1.1. CCE

By examining the CCE and its relationship with the STBR (Fig. 3), it becomes apparent that it is negative for both bed materials studied. The CCE drops by roughly 4% when the STBR increased from 0.8 to 1 and from 1 to 1.2 for F054. For F046 the effect of reducing the STBR is less apparent, since the drop was only 1% between the 0.8 and 1.2 STBR set points. In general, a higher steam supply is expected to promote the water-gas shift (WGS) reaction as well as carbon (heterogeneous WGS), methane and tar reforming, mainly to CO and H_2 [38,39]. Therefore higher carbon conversions were expected for increasing STBR at least until a certain point. When very large amounts of steam are introduced in a steam reformer at temperatures lower than the operating temperature, the temperature of the bed also drops. This leads to a subsequent decrease of the carbon conversion efficiency [40]. In the IHBFBSR, temperature is controlled according to a set point, so such a behaviour would not be noted by the temperature readings. An indirect way to evaluate the system's behaviour is through the operation time of the bottom burner, which can provide a correlation between STBR and the power supplied to the system. From Table 3, it can be concluded that for both F054 and F046 experiments, a significant decrease in the operating time of the bottom burner for a STBR of 0.8 took place, compared to 1.2 and 1. This indicates that for lower STBR the heat requirement of the process is lower. Since the amount of biomass feed and the λ are the same for all these experiments, that behaviour can be attributed to a lower carbon conversion efficiency. The total amount of char produced from the steam/air experiment corresponds to the amount of carbon residue of the steam reforming process that was not converted through the oxidation reactions with air. For lower STBR, reduced char

Table 3
Percentage of actual operating time for the bottom and top IHBFBSR burner for the various STBR steam/air gasification experiments conducted with PG as feedstock.

	Bed Material				
	F054			F046	
STBR	1.2	1	0.8	1.2	0.8
Bottom burner on (%)	96.3	96.7	81.3	86.5	73.1
Top burner on (%)	84.4	82.3	91.4	91.7	91.1

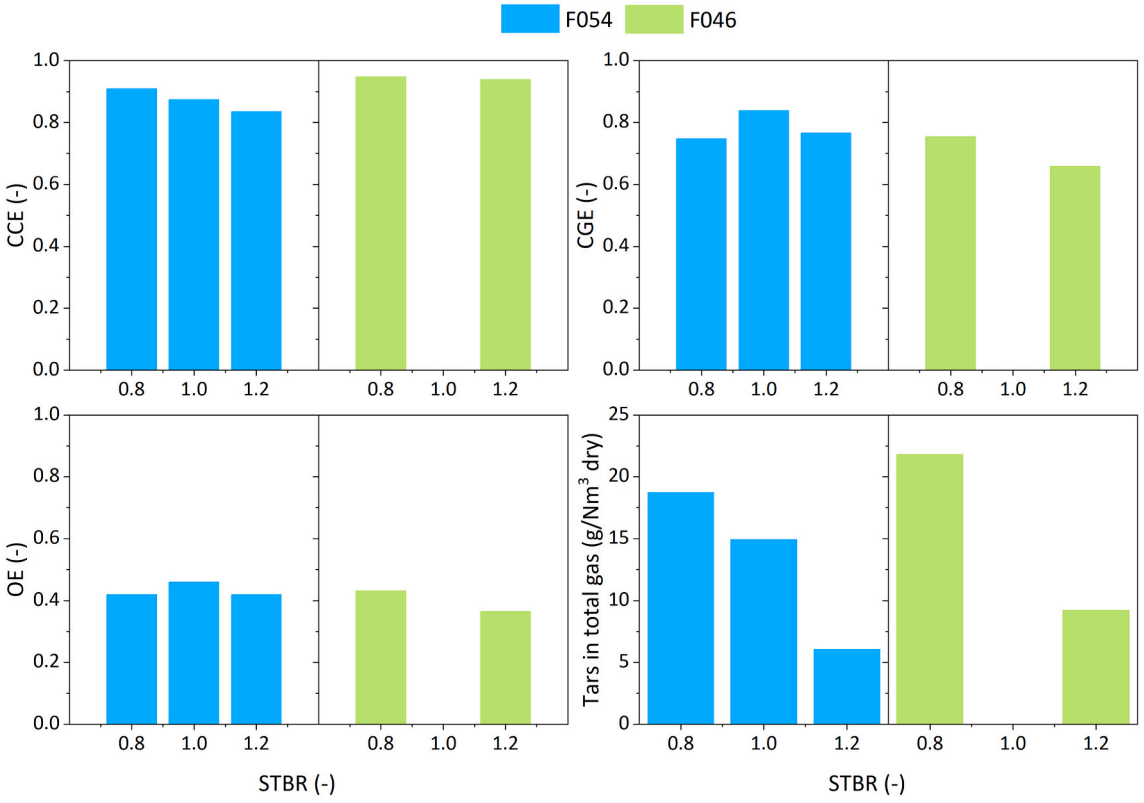

Fig. 3. Effect of STBR and bed material particle size on the CCE (top left), CGE (top right), OE (bottom left) and tar content (including benzene) in the product gas for PG steam/air gasification with λ = 0.2 at temperatures between 830 °C and 840 °C in the IHBFBSR. Corresponding experimental indexes: 1,2,3,4 and 5 (SP2).

conversion by steam, leaves more carbon available for the exothermic oxidation reactions. This can lead to reduced heat requirements and increased CCE values for lower STBR, explaining the contradiction of the latter with literature. The lower fluidization velocity/gas residence time imposed with lower STBR, since the biomass and air flow remain constant, add to this effect.

Carbon conversion appears to be promoted by employing a larger particle size (87% versus 94% on average, in favour of F046). However, as it has also been reported in [41], smaller bed material particles increase the turbulence in the bed (higher particle-related Reynolds numbers) leading to improved heat and mass transfer in the area and therefore higher carbon conversion. Additionally, it should be mentioned that for Geldart B particles, such as in this case, the bubble size is independent of the particle size [42], so this aspect of hydrodynamics does not offer any explanations for the observed behaviour. Furthermore, slightly higher bed temperatures (~6 °C on average) and lower initial freeboard temperatures (by 11 °C on average) were reported for the smaller bed material particle size experiments. The latter observation showcases improved heat transfer capabilities although the difference in temperature is not that large. The improved heat transfer is also evident by the reduced operating time of the bottom burner for F046, as shown in Table 3. Consequently, the higher carbon conversion noted for the F046 experiments compared to using F054, can be attributed to experimental error in char collection. Alternatively, it can be hypothesized, that the improved heat and mass transfer for the F054 experiments, increases the accessibility of the char particles, thus increasing the tar cracking capabilities of the char bed inventory. This could lead to enhanced secondary coking and therefore higher char yields.

4.1.2. CGE, OE and gas composition

In regards to CGE and OE, where the differentiating factor among the various experiments is the LHV value of the product gas, no clear trends or correlations emerge. Overall, for the F054 steam/air gasification experiments with PG, the average CGE was 78.4% and average OE was 43.3%. The higher CGE value noted for the STBR = 1 / F054 experiment can be attributed to the lower N_2 content of the product gas of this experiment by roughly 2 vol% compared to the experiments with STBR of 1.2 and 0.8. The corresponding values for the F046 experiments with PG (which were two instead of three) were 70.6% and 39.8%, for CGE and OE, respectively. As it was the case for the STBR = 1 / F054 experiment before, also here the low values for the STBR = 1.2 / F046 are outliers, due to a much higher N_2 content in the product gas. In Fig. 4, the dry nitrogen free (dnf) composition of the gas produced, is presented for both F054 and F046 bed material sizes. For both cases, a positive correlation of STBR with H_2 and a negative one with CO is established. For CH_4, a drop is observed, namely 0.4 vol% dnf on average for F054 and 0.7 vol% dnf for F046. However, the short range of experimental points (three for F054 and two for F046) along with the low magnitude of the drop, do not allow drawing any concrete conclusions from this observation. Overall, such trends were highly anticipated, since the WGS, CH_4 reforming and tar reforming reactions are promoted by the addition of more steam [43]. Regarding the differences between the two bed materials employed, it can be noted that while CH_4 production was quite similar for both, the increase in bed material size, seemed to lead to lower H_2 and higher CO and CO_2 yields. Overall, the improved heat and mass transfer imposed by the increased turbulence in a system employing lower bed material sizes compared to higher ones, has been reported to lead to increased catalytic activity in the case of olivine bed material in favour of H_2 production [41]. The corundum bed material employed in this work is expected to be inert. However the char that is produced and accumulates in the bed can act as a catalyst for reforming or cracking reactions of hydrocarbons and its presence in general promotes tar destruction and syngas production [44]. Therefore it can be argued that the increased turbulence of the system when lower bed material particle sizes are employed, enhances interaction with char particles that promotes tar conversion. It has been shown in literature [45], that aromatic compounds can decompose over the char surface due to coking, forming also H_2 in the process. In general, char's catalytic activity is dependent on its pore size, surface area as well as on its mineral content [46]. By decreasing the bed material particle size employed and thus increasing the turbulence of the system, the char surface area available for tar elimination reactions becomes larger due to the lager accessibility of the char particles.

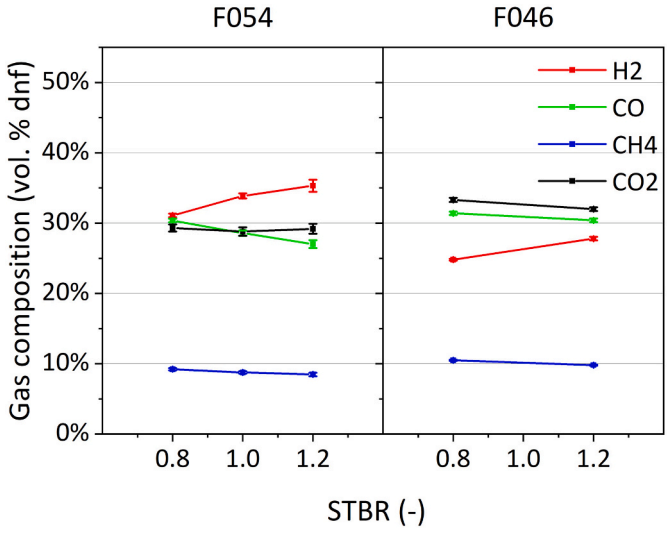

Fig. 4. Effect of STBR and bed material particle size on the composition of gas produced from PG steam/air gasification with λ = 0.2 at temperatures between 830 °C and 840 °C in the IHBFBSR. Corresponding experimental indexes: 1,2,3,4 and 5 (SP2).

4.1.3. Tar and benzene composition

The increasing STBR leads to a significant decrease of the amount of tars produced for both cases of bed material studied (Fig. 3). For F054, from a 19 g/Nm^3 dry concentration for a STBR of 0.8, the tar in total gas content dropped to roughly 6 g/Nm^3 dry for a STBR of 1.2. The corresponding drop for the F046 experiments was similar, namely from 22 g/Nm^3 dry at 0.8 to 9 g/Nm^3 dry at 1.2. In general, the increase of the STBR leads to the enhancement of tar reforming reactions for the production of H_2 and CO, an effect very well described in literature [47,48]. This observation is also consistent with the previous remarks regarding H_2 formation intensification with increasing STBR. The individual tar compounds formed at each case are presented in Fig. 5. Benzene production is included separately since it is not considered a tar species and is by far the most abundant condensable product compound detected.

The increase in STBR leads to a decrease of both the amounts of benzene and naphthalene formed. Naphthalene belongs to the light polyaromatic tars category [49], constituting its main representative in terms of abundance in this work and the second most abundant condensable specie formed after benzene. Overall, the increase of STBR led to a decrease in the heterocyclic (phenol), light aromatic (toluene, ethyl benzene) and light polyaromatic tars (naphthalene, acenaphthylene, fluorene, anthracene, phenanthrene). The only exception was noted for the case of heterocyclic (phenol) tars for F046. According to Jess [50], the effect of steam on aromatics conversion can be considered as minimal. Furthermore, it has been suggested that the presence of H_2 inhibits the conversion of benzene and naphthalene in particular [50] or even PAH in general [51]. More specifically, despite the fact that the presence of H_2O increases the tar decomposition rate, the presence of H_2, whose yield is positively correlated to H_2O, depresses the tar decomposition rate. The H_2 reacts with radicals generated to form a stable tar molecule and a hydrogen radical, thus leading to higher concentrations of smaller, more stable PAHs, such as naphthalene and benzene [52]. This effect is

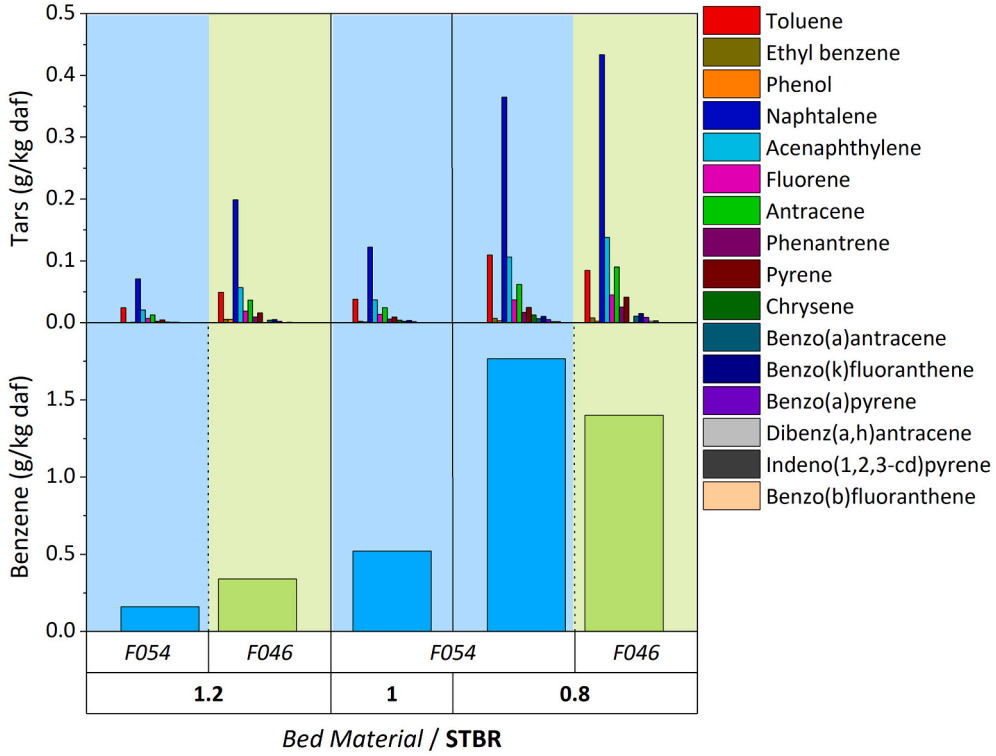

Fig. 5. Effect of STBR and bed material particle size on the benzene and tar compounds production per kg of d.a.f. PG feed, for steam/air gasification with λ = 0.2 at temperatures between 830 °C and 840 °C in the IHBFBSR. Corresponding experimental indexes: 1,2,3,4 and 5 (SP2).

not presented in the steam gasification experiments with PG presented here, since both benzene and naphthalene yields decrease with increasing steam supply. In regards to the total tar yield, its negative correlation with STBR has been reported in literature [48,51]. Correlations between temperature and the efficiency of tar suppression, as well as the selectivity towards lighter compounds and the increase of STBR have also been reported in [53]. It has also been argued, that the presence of steam does not influence aromatic tar yields, as far as no catalyst of temperatures above 1100 °C are employed [54]. For benzene in particular, it has been reported that its decomposition rate is independent of steam concentration [55]. Finally, Qin et al. [56], argue that enhanced production of H radicals at high temperatures during steam gasification can lead to stabilization of tar intermediates and thus prevent their polymerization to aromatic compounds. Therefore, the reason for the observed major reduction in benzene and naphthalene yields for increasing STBR can be attributed to the catalytic activity of the char accumulating in the bed area, promoting benzene and tar steam reforming.

Furthermore, a 3 g/Nm^3 difference in tar production (Fig. 3), was observed between the two bed materials for STBRs of 0.8 and 1.2, with the larger particle size bed material (F046) presenting the higher values. For both STBR values studied, the PAH (light and heavy) yield was significantly higher for the F046 experiments. However, for the STBR = 0.8 experiments, the BTEX content (xylene was not measured) was higher for the F054 experiments (Fig. 5). The improved heat and mass transfer, due to the turbulence increase of the system, appears to promote tar destruction. Tar production was probably reduced through the increased catalytic activity of the char particles accumulating in the bed, when the smaller (F054) bed material results are compared to the coarser's ones (F046). The higher BTEX yield observed for F054 in the case of STBR of 0.8 can be attributed to the more intense formation of those products through PAH cracking [50] compared to the case of F054.

4.2. *Effect of λ – High temperature (HT) versus low temperature (LT) experiments*

In this section the F046/ExR experiments with experimental indexes 7 (SP2) and 8 (SP2) are compared. The two most pronounced effects of λ reduction concern the temperature of the system as well as the increased char accumulation in the bed area. In particular, for the two experiments discussed in this section, with the decrease of λ from 0.2 to 0.04 the average bed temperature (TC01 – TC03) dropped from 833 °C to 711 °C and the maximum freeboard temperature from 878 °C to 825 °C. The average freeboard temperature dropped from 865 °C to 804 °C, while the location of the maximum point moved from TC05 to TC06.

4.2.1. *CCE, CGE and OE*

The reduction of λ, expectedly led to lower carbon conversion levels (89% versus 82%) (Fig. 6). The char mass obtained through the bed sieving process was a factor 8 times higher for the LT experiments (0.04 kg/kg of feed versus 0.005 kg/kg of feed). Overall, the decrease in CCE for lower λ and temperatures, was expected since both factors enhance char oxidation and in general the breakdown of biomass molecular bonds [40]. Regarding CGE, it increased by 4% for the decrease of λ, due to the increase of the product gas LHV from 4.9 MJ/Nm^3 to 6.4 MJ/Nm^3, but also due to the lower amount of ExR feed employed (8 kg/h for LT versus 10 kg/h for HT). On the contrary, the OE of the system decreased for lower λ values. This reversal of the behaviours for the OE compared to CGE, is attributed to the fact that the bottom burner was on for 95% of the time for the HT experiment compared to the LT experiment where it was on constantly. This corresponds to a power input difference of ~3.4 MJ, leading to the slight increase of the overall efficiency for the high λ and temperature experiment, despite the fact the LHV of the product gas is significantly lower in this case and a higher biomass feeding rate was employed. In regards to the LHV, its value increased for lower λ values, apparently due to less effective dilution of the product gas with N_2, considering that the CO concentration was actually lower and the one of CH_4 practically the same for the LT (λ = 0.04) experiment.

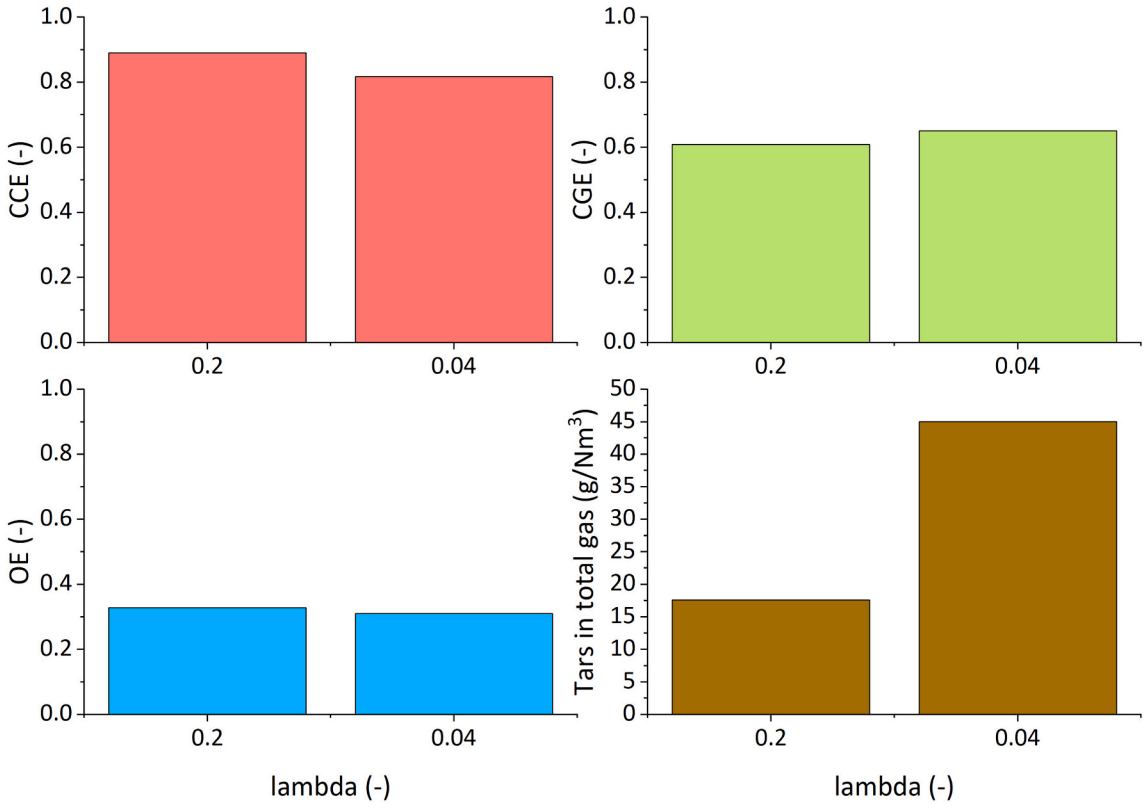

Fig. 6. Effect of lambda (λ) on the CCE (top left), CGE (top right), OE (bottom left) and tar content (including benzene) in the product gas for ExR steam/air gasification with STBR = 1.2 in the IHBFBSR. Corresponding experimental indexes: 7 and 8 (SP2).

4.2.2. Gas, tar and benzene composition

In the graphs of Fig. 7, the volatile products of ExR steam/air gasification LT and HT experiments are presented. The reduction of λ, led to an increase of the H_2 yield by ~12 vol% dnf. The CO and CO_2 yields decreased by 7.5 and 4 vol% dnf, respectively, while the CH_4 yield was not affected. The N_2 concentration of the product gas was significantly reduced, namely from 57 vol% to 46 vol% dry. It should also be mentioned that the total gas yields of the two experiments were very similar (0.99 and 1.01 Nm^3/kg daf for the HT and LT experiment, respectively). On the other hand, the water content in the produced syngas increased from 28 vol% for the HT to 47 vol% for the LT experiment. In regards to total benzene and tar formation (Fig. 6), the reduction of λ and temperature, led to much higher overall yields. Tar content in the gas product (including benzene) increased from 17.6 g/Nm^3 to 45 g/Nm^3 for the reduction of λ from 0.2 to 0.04. Benzene was the most abundant condensable specie detected by a huge difference, while naphthalene, acenaphthylene, toluene, anthracene and fluorene followed in roughly that order. The yield of each individual compound studied, increased by at least three times for the decrease in λ value, with the exception of ethyl benzene which was not influenced by this change. The most pronounced effect was evident on the yields of phenol and toluene. More specifically, the phenol yield was 14 times and the toluene yield 7 times higher for the LT experiment compared to the HT one.

Since steam reforming reactions are endothermic, the reduction of the reactor temperature as an indirect effect of λ reduction leads to less H_2O and carbon reforming, as it was also evident by the decrease of CCE [57]. Consequently, H_2O and char yields are higher for lower λ, as it was the case in this work. Another effect of the lower system temperature, especially in the bed area, is the steep increase of the phenol yield. Despite phenol not being one of the most abundant tars in these experiments, its presence in the product gas is indicative of the performance of the IHBFBSR in terms of tar removal efficiency. In general, lower temperatures favour the formation of tar species such as phenol and toluene, with diversified substituent groups [58]. The present results illustrate, that despite the fact that for the LT experiments, the average temperature of the freeboard is around 804 °C, it does not suffice for cracking of such products. Of course, the reduced amount of air in the system compared to the HT experiments enhances this particular behaviour, due to the limitation of tar oxidation reactions. For benzene, its yield for the LT experiment was 2.5 times higher than for the HT experiment. In general, higher temperature and lambda values reduce the total amount of tars produced but also lead to an increased aromatisation (PAH and BTEX formation) [58,59]. However, in the LT experiments, the operating temperature and/or oxidative media availability does not suffice for the decomposition of heavier tars to more stable compounds such as benzene and naphthalene. Consequently, benzene formation comes mainly from primary pyrolysis products decomposition in this case. For HT experiments where both pathways for benzene formation are available, the lower yields indicate its decomposition at least to a certain degree. Therefore, it can be argued that in the context of the IHBFBSR, benzene production is largely dependent on the temperature and/or oxidative media presence. Naphthalene and PAH yields in general are significantly higher for the LT experiment despite the fact that their production is expected to be fairly limited at temperatures close to 700 °C [53,60,61]. Therefore, one would expect that the amount of PAH produced from the LT experiments would be less than for the HT ones, considering the aforementioned remark. As it mentioned by Milne et al. [61] the addition of oxygen at low temperatures can accelerate the destruction of primary pyrolysis products (levoglucosan, hydroxyacetaldehyde, furfurals, etc.), but it has a minimal effect on benzene and secondary (phenolics, olefins) and tertiary products (BTEX, PAHs) destruction. Therefore, the presence of oxygen is not the deciding factor in this situation since temperature is supposed to be the limiting factor in the formation of PAH. Considering these observations, two different, however non-mutually exclusive hypotheses can be made regarding the higher amount of PAH produced

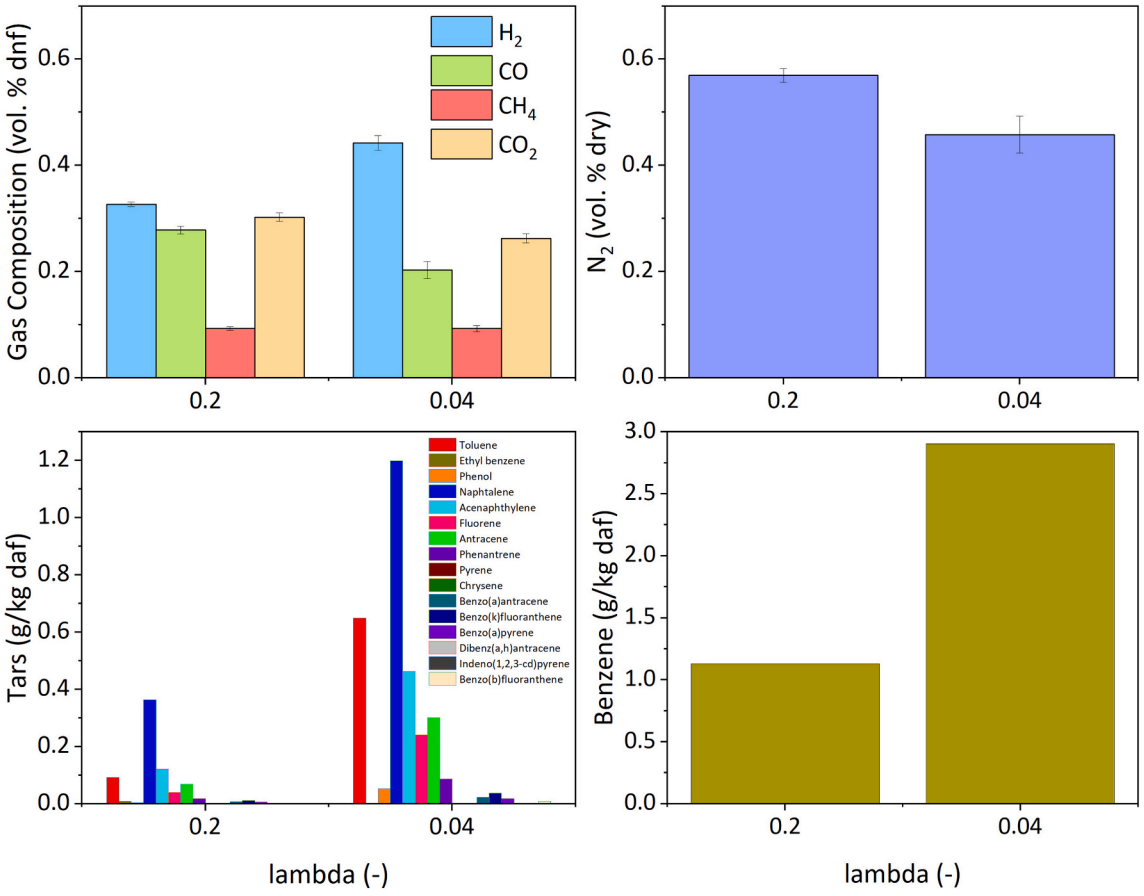

Fig. 7. Product gas composition (top left), N_2 yield (top right), tar yield (bottom left) and benzene yield (bottom right) for steam/air gasification of ExR with STBR = 1.2 in the IHBFBSR for different values of lambda (λ). Corresponding experimental indexes: 7 and 8 (SP2).

from the LT compared to the HT experiments. The first one is that PAH formation for LT experiments takes place in the freeboard where the temperatures are higher rather than in the bed area. The second hypothesis is based on the catalytic effect of the accumulated char bed, which was already presented for the PG experiments presented in Section 4.1. Therefore, it can be hypothesized that the presence of char in the bed could lead to PAH formation at lower temperatures than usual.

Regarding H_2, it was expected that its yield would be negatively influenced by the reduction of the process temperature. H_2 production is generally favoured by high temperatures that promote endothermic char gasification and steam reforming and/or cracking of light hydrocarbons and tars [40,48]. Furthermore, its production is also linked to tar secondary reactions [60], that for the LT experiments appear to be less active. However, elevated values of λ can also increase H_2 partial combustion rate [40]. Therefore, it can be argued that H_2 production in HT experiments is severely reduced by the combined effect of partial oxidation and the high temperature of the freeboard (865 °C on average). The fact that the H_2 yield is significantly higher for the LT and low λ experiments points to this direction. Regarding the rest of the gases, the increase of CO_2 for higher λ can be attributed to the enhancement of char, CO and CH_4 oxidation reactions [2]. On the other hand, CO values despite being expected to drop for higher λ due to increased partial oxidation [62], showed an increasing trend. This can be potentially attributed to the increased CCE for higher λ/ temperature experiments, which hints to the formation of CO through char partial combustion [2]. Additionally, it is also possible that homogeneous tar conversion, can also be responsible for the increased CO formation in this particular case [60].

4.3. *Effect of secondary air injection*

In this section, the effect of the injection of air in the freeboard is going to be examined for both bed materials (F046 and F054) studied in this campaign. The LT/ExR experiments which were studied in that regard, correspond to the index numbers 8 to 12 as described in Table 2. Overall, the experiments described in this section were performed with 0, 4 and 8 kg/h of secondary air injected. The addition of 4 kg/h and 8 kg/h of secondary air, corresponds to overall lambda ($\lambda_{overall}$) values of 0.13 and 0.21, respectively. These values were calculated using Eq. (2) and considering both the air injected through the bottom of the IHBFBSR and the freeboard. For the F046 experiments the increase of the amount of secondary air led to the increase of the average freeboard temperature (TC04 – TC07) (804, 807 and 814 °C, respectively). The magnitude of the observed differences is low, because TC04 is included in this calculation. For the LT experiments, the increased char accumulation in the bed leads to the expansion of the "bed" area to include also TC04. This explains the overall low average freeboard temperature, since the "char bed" is included in it. If just the last two thermocouples are

considered (TC06 – TC07), which correspond to locations above the secondary air injection point, the corresponding temperature values show the actual changed imposed on the system (818 °C for 0 kg/h versus 857 °C for 4 and 8 kg/h). The respective values for F054 are slightly lower in terms of TC04 – TC07 average (796 °C and 805 °C for 4 and 8 kg/h respectively) and 848 °C – 856 °C for the TC06 – TC07 average. Overall, the average bed temperature for the three F046 experiments was 708.6 °C, roughly 10 °C lower from the corresponding value of the two F054 experiments (Table 2). In the previous comparison of the effect of bed material particle size on the temperature of the TC01 – TC05 area of the IHBFBSR (Section 4.1) similar conclusions were derived. Namely, the increased turbulence of the system due to the smaller particle size of the bed material for F054 leads to improved heat and mass transfer, which in its turn leads to smaller differences in temperature between bed area and early (TC04 – TC05) freeboard. This leads to a higher bed and lower initial freeboard temperature for the F054 steam/air gasification experiments with ExR, by 10 °C and 23 °C respectively on average, compared to the F046 experiments.

4.3.1. CCE

The CCE values for F046 (coarser) were similar to F054 for 4 kg/h of secondary air, but they were ~3.5% higher for 8 kg/h (Fig. 8). This result is fairly consistent with the corresponding results of Section 4.1, however the magnitude of the observed differences is significantly smaller. For CCE, a slight increasing trend for increasing amounts of secondary air was noticed in both cases, most notably in the case of F046 were the value rose from 82%, to 83% and 88%, respectively. In both cases of bed material particle size, the amount of char collected through the bed sieving process was not particularly affected by the secondary air injection, as it was expected. However, the total amount of fines in the bed and cyclones decreased significantly for increasing secondary air injection. For F054, a drop of 15% was noted in the amount of fines produced from 8 kg/h of secondary air compared to the 4 kg/h case. For F046, the corresponding drops were 19% and 67% from 0 to 4 kg/h and 4 to 8 kg/h, respectively. Therefore, it can be argued that the introduction of secondary air leads to partial char oxidation reactions in the freeboard, reducing the amount of char collected in the cyclones and thus improving carbon conversion.

4.3.2. CGE and OE

Regarding CGE and OE, contradictory results are obtained from the experiments conducted with the two different bed materials. For the F046 experiments, the increase of the amount of secondary air employed led to lower CGE and OE values, while the opposite behaviour was observed for the F054 experiments. For both cases, LHV values decreased for increasing amounts of secondary air, mostly due to dilution of the product gas with N_2. In particular, for the F046 experiments the LHV fell from 6.4 MJ/Nm^3 dry, to 4.9 and 4 MJ/Nm^3 dry, when the secondary air injection was changed from 0 to 4 and 8 kg/h, respectively. The corresponding values for F054 were 5 and 4.3 MJ/Nm^3 dry for 4 and 8 kg/h, respectively. Considering this trend for the calorific value of the product gas, the observed behaviour of the CGE and OE can be attributed to its actual yield. For the F054 experiments the dry-N_2-free gas yield was favoured by the increase in the amount of secondary air injection, rising from 0.94 to 1.05 Nm^3 dnf/kg daf. On the contrary, in the case of F046 the dry-N_2-free gas yield decreased from 1.01 Nm^3 dnf/kg daf for no secondary air added, to 0.92 and 0.87 Nm^3 dnf/kg daf, for 4 and 8 kg/h, respectively.

4.3.3. Gas composition

The effect of secondary air injection and bed material particle size on gas composition is presented in Fig. 9. The aforementioned increase of the gas yield in the case of the F054 steam/air gasification experiments, for increasing amounts of secondary air injection, in contrast to F046, can be attributed to the improved tar conversion achieved with F054, especially when the two respective 8 kg/h secondary air injection

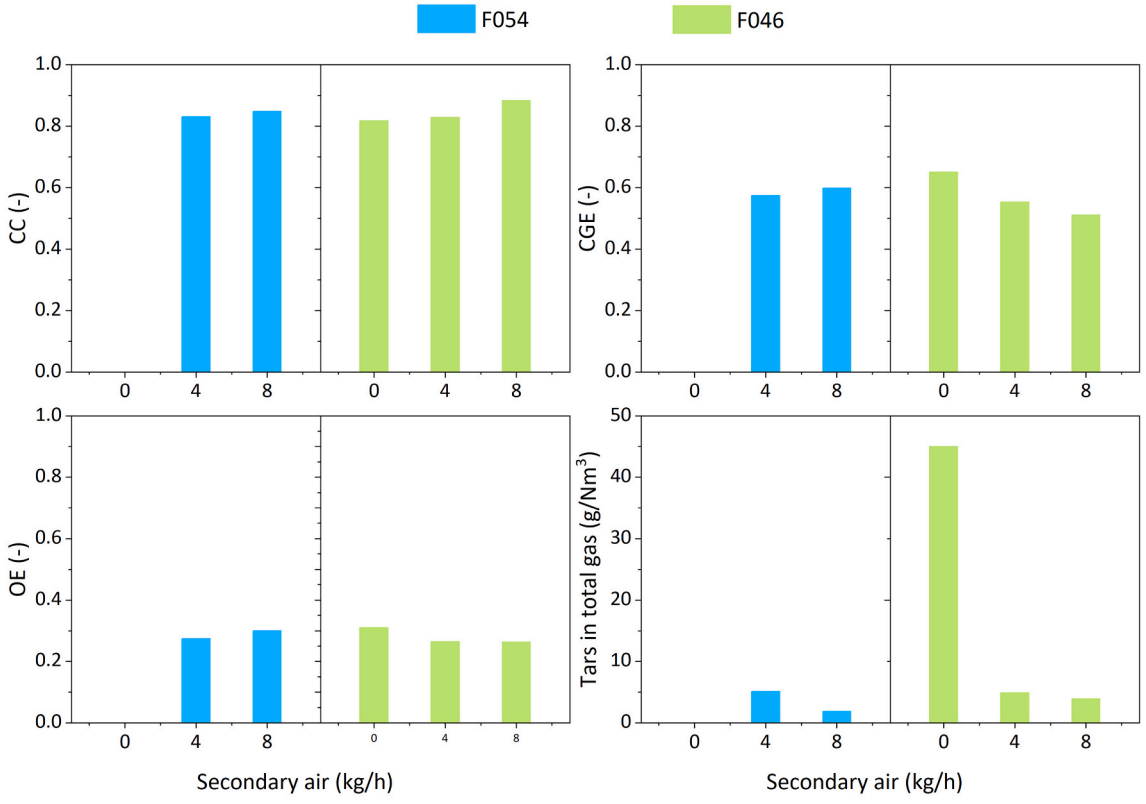

Fig. 8. Effect of secondary air injection and bed material particle size on the CCE (top left), CGE (top right), OE (bottom left) and tar content (including benzene) in the product gas for ExR steam/air gasification with λ = 0.04 and STBR = 1.2 in the IHBFBSR. Corresponding experimental indexes: 8, 9, 10, 11 and 12 (SP2).

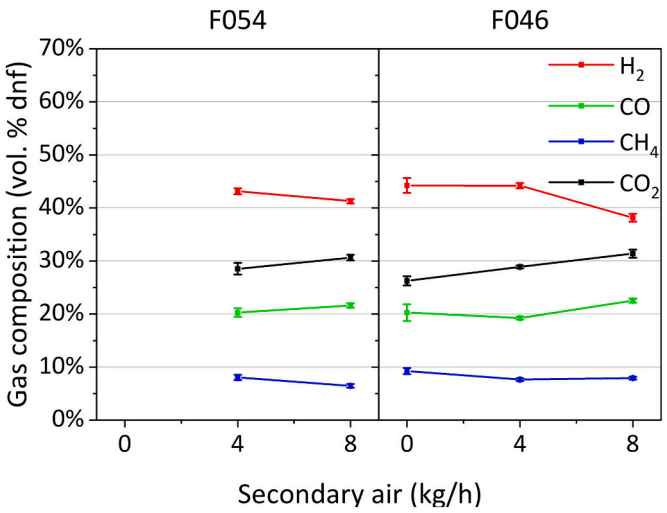

Fig. 9. Effect of secondary air injection and bed material particle size on the composition of gas produced from ExR steam/air gasification with $\lambda = 0.04$ and STBR = 1.2 in the IHBFBSR. Corresponding experimental indexes: 8, 9, 10, 11 and 12 (SP2).

experiments are compared. The F054 experiments showed better tar conversion (Figs. 8 and 10), similarly to the previously presented PG experiments in Section 4.1. The increased turbulence of the system for lower bed material particle sizes (F054), enhances interaction with char particles that accumulate in the bed promoting tar conversion. When comparing the 8 kg/h secondary air injection experiments in terms of dry product gas, the N_2 in the F054 experiments is roughly 4 vol% lower than for F046. The opposite behaviour is found for H_2, CO and CO_2. In particular, the corresponding yields were higher for F054 compared to F046 by approximately 3 vol%, 0.6 vol% and 1 vol%, respectively. As previously discussed, H_2 and CO are considered as direct products of tar cracking/reforming reactions, which explains the observed difference. The difference in CO_2 could be due to the occurrence of CO oxidation reactions to a larger extent for the F054 experiments, following its aforementioned increased production. Overall, the improved tar cracking capabilities of smaller corundum bed particle sizes was also proven here. Nevertheless, in terms of the dry-nitrogen-free gas composition, the differences between the bed material sizes were marginal, with the exception of H_2.

When studying the effect of secondary air injection in the dry-N_2-free gas composition, it is clear that it had a negative impact mostly on the H_2 and to a lesser extent on the CH_4 yield. On the contrary, CO and CO_2 yields were positively influenced by the increase of the amount of secondary air introduced. The reduction of the combustible gases yields was expected due to the addition of the secondary air [63,64], however this was not seen for CO. Therefore, it can be suggested that the enhancement of CO production from tar cracking/reforming as well as from the Boudouard and carbon oxidation reactions, as it is suggested by the higher CCE values, overcomes the increased effect of CO combustion. Furthermore, it is apparent, that the transition from 0 kg/h to 4 kg/h of secondary air had no influence at all in the H_2 yield for the F046 experiments. Apparently, the increased H_2 combustion rate is matched by the increased production though tar cracking and reforming reactions, due to the more reducing environment and the higher temperatures achieved.

4.3.4. Tar and benzene composition

The overall positive effect of secondary air addition on tar reduction, due to the oxidative atmosphere and the elevated temperatures achieved in the freeboard (Fig. 8), has also been reported in the literature [63–66]. Its effect on specific compounds is presented in Fig. 10. With the exception of benzene for 4 kg/h of secondary air, the amount of tars and benzene produced from steam/air gasification with corundum F054 were lower than in the F046 experiments, in a behaviour consistent with the HT experiments presented in Section 4.1. In regards to the effect of the secondary air injection, for the F046 experiments, the overall tar yield decreased by ~90%, regardless of the amount. This drop corresponds to a reduction from ~1 vol% (45 g/Nm^3) of the total dry gas to 0.11 vol% (5 g/Nm^3) and 0.09 vol% (4 g/Nm^3) for 4 kg/h and 8 kg/h of secondary air, respectively. For F054, with the increase of the amount of air injected from 4 kg/h to 8 kg/h the total amount of tars and benzene produced, decreased by 63 wt% to 1.9 g/Nm^3.

As it was also the case for the HT / PG and ExR steam/air gasification experiments, benzene was by far the most abundant condensable species detected. The injection of secondary air (4 kg/h) with F046 as a bed material led to benzene's yield reduction by 88 wt% compared to the no secondary air case. With the increase to 8 kg/h for F046, a 17 wt% reduction of benzene's yield was observed, with the corresponding decrease for F054 being almost three times higher. Naphthalene, acenaphthylene, anthracene and toluene were the most abundant tar species formed, with naphthalene presenting the higher concentrations by far. Its yield was reduced by 64% with the increase of secondary air amounts from 4 to 8 kg/h for F054. For F046, the increase from 0 kg/h to 4 kg/h and finally to 8 kg/h led to a reduction by 87 wt% and 28 wt% of the naphthalene yield. In terms of tar classes, heterocyclic tars (phenol), were reduced by 92% and 77% for an increase of secondary air injection from 4 kg/h to 8 kg/h for F054 and F046, respectively. The amount of light aromatics and light polyaromatics also decreased with increasing amounts of secondary air. The latter effect, was more pronounced for F054, where the anthracene yield was reduced by roughly 97%, while phenanthrene disappeared completely absent from the 4 to 8 kg/h steam/air gasification experiment. The reduction especially of light aromatic and light PAH has also been reported in the literature for secondary air injection systems [66]. Considering heavy polyaromatic tars, while for the F054 experiments their yield dropped by 90% from 4 kg/h to 8 kg/h of secondary air, in the case of F046, after an initial drop of 93% from 0 to 4 kg/h, their yield increased by 60% when the secondary air injection was further increased to 8 kg/h. This was mostly due to a steep increase of the pyrene yield by ~60 times. Such an observation for the effect of secondary air injection on heavy PAH was also made in [67] with no clear indication on the reasons behind it. Pyrene is a product of naphthalene decomposition and constitutes a stable PAH without substituent groups [50,68]. Therefore the increase of its yield might be attributed to the decomposition of mainly naphthalene [69], which can be found among the gasification products in higher amounts for F046 rather than F054 bed material. It should be mentioned, that the low amounts of heavy PAH detected, lead to a very high potential influence

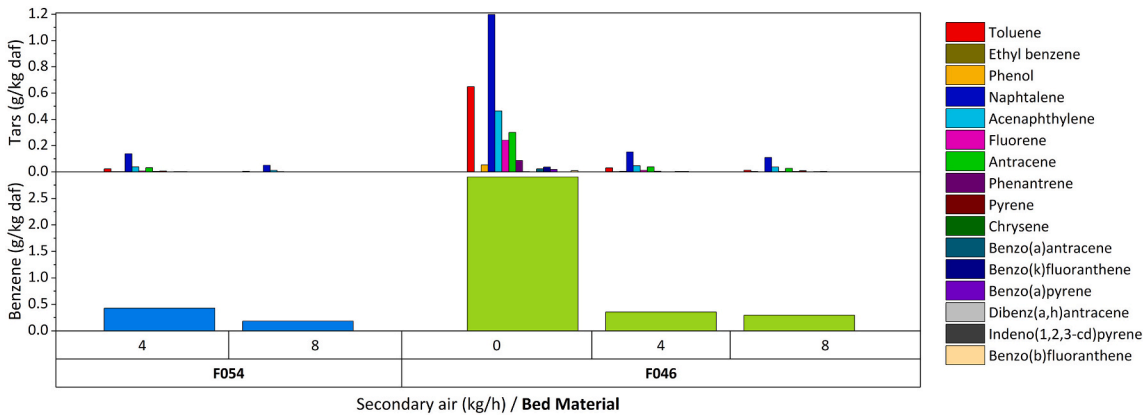

Fig. 10. Effect of secondary air injection and bed material particle size on the benzene and tar compounds production per kg of d.a.f. ExR feed for steam/air gasification with $\lambda = 0.04$ and STBR = 1.2 in the IHBFBSR. Corresponding experimental indexes: 8, 9, 10, 11 and 12 (SP2).

of an experimental error on the values discussed here. Overall, it can be argued, that the injection of secondary air appears to be a very efficient method for tar removal in the context of the IHBFBSR, regardless of the class.

4.3.5. *Overview of the effect of secondary air injection*

In general air injection, either primarily or secondarily, led to the increase of the bed temperature of the IHBFBSR, due to increased char and biomass oxidation (Table 4). However, the effect of its addition on the average TC06-TC07 temperature on the freeboard is negligible. Therefore, it can be argued that the difference in terms of the temperature profile between the two methods of supplying air, lies mostly on how wide the high temperature zone is and on the location of the maximum. However, another effect of the reduction of the primary air is the increased accumulation of char in the bed area. As it is evident by the readings of TC04, the temperature at this region is slightly above the average bed temperature. The reduction of primary air leads to lower CCE values, despite the fact that secondary air injection improves the secondary conversion of fine char particles in the freeboard. The effect of secondary air addition on the gas yield (dnf) is negative. Despite the fact that lower amounts of total air are introduced and therefore dilution by N_2 is reduced, the lower degree of char conversion plays a significant role on the amount of gas produced. For example, the carbon content in the product gas was 1.2 kg dry less for experiment 9 compared to 7. The negative effect of secondary air addition on the gas yield is also reflected on the OE values (Table 4). However, the LHV of the product gases can be viewed as comparable, between the cases of 4 kg/h secondary air injection and 11.3/0 kg/h of primary/secondary air. At this level, the effect of N_2 dilution is apparently evened out by the increased tar conversion due to the catalytic char bed and localised air supply. This "dedication" of the air supplied to the system to tar conversion along of course with the effect of the char bed, is reflected on tar content in the product gas. Despite the fact that less air is injected for experiment 9 (and of course 10), the tar content is significantly lower. Additionally, the H_2/CO ratio is improved by the reduction of the primary and the addition of secondary air. Conclusively, the negative effect of secondary air addition on the syngas quality, can be mitigated through the employment of moderate amounts of air ($\lambda_{overall} \approx 0.13$) and the catalytic effect of accumulating char, as it was previously suggested also in [66]. Furthermore, the results presented both here and Section 4.1, strongly suggest that the employment of smaller (F054) bed material particle size can lead to improved quality of the produced syngas.

4.4. *Effect of steam/air gasification duration*

For the experiments where tar sampling was performed twice, the first sampling point (SP1) was initiated after switching from the combustion/warming up regime, to steam/air gasification. The second sampling (SP2), was performed after a steady state was achieved. The main purpose of performing both samplings, is to investigate the effect of char accumulation in the bed. For HT experiments (5,6 and 7), the temperature of the entire system increased with time (Table 5). For HT experiments, char accumulation still occurs at the bed, however to a much lower extent compared to the LT experiments, due to its partial oxidation. On the contrary, for the LT experiments the average bed temperature decreases between SP1 and SP2. The behaviour for the TC04 – TC05 region was similar, with the temperature increasing with time for the HT experiments and decreasing for the LT ones. Increased char accumulation for the LT experiments leads to comparatively lower temperatures for TC04, which tends to become equal to the one of the corundum fluidized bed right below. Finally, regarding the TC06 – TC07 average temperature, its value increased in all cases, with the exception of 8 kg/h of secondary air injection. In this case, the temperature in this region of the freeboard was at roughly the same levels throughout the entire the experiment.

4.4.1. *Gas composition*

Accumulation of char in the bed, appears to be beneficial for the gas yield, with the average increase, despite only marginal in some cases, being ~0.15 Nm^3 dnf/kg daf. The enhanced catalytic activity of the char

Table 4
Comparison of the effect of the total amount of air introduced and the respective introduction method for steam/air gasification experiments in the IHBFBSR, with a STBR of 1.2, ExR as a feedstock and corundum F046 as a bed material.

Index (#)	Primary/ secondary air (kg/h)	Average bed temperature/ TC04/Average TC06-TC07 (°C)	Overall λ (–)	CCE (–)	Gas Yield (Nm^3 dnf/ kg daf)	LHV product gas dry (MJ/ Nm^3 dry)	OE	H_2/ CO	Tars in total gas (g/Nm^3)
7	11.3/0	833/865/859	0.23	0.89	0.99	4.90	0.33	1.2	17.6
9	1.9/8	704/745/857	0.21	0.88	0.87	3.96	0.26	1.7	3.9
10	1.9/4	710/731/857	0.13	0.83	0.92	4.86	0.26	2.3	4.9
8	1.9/0	711/775/818	0.04	0.82	1.01	6.44	0.31	2.2	45

Table 5
Effect of steam/air gasification duration in the IHBFBSR on various process parameters and product yields (experiments 5–8).

Index (#)	5		6		7		8	
Set Point	SP1	SP2	SP1	SP2	SP1	SP2	SP1	SP2
Bed Material	F046	F046	F054	F054	F046	F046	F046	F046
Biomass	PG	PG	ExR	ExR	ExR	ExR	ExR	ExR
λ(−)	0.20	0.20	0.23	0.20	0.23	0.20	0.04	0.04
STBR (−)	0.8	0.8	1.2	1.2	1.2	1.2	1.2	1.2
Sec. air (kg/h)	0	0	0	0	0	0	0	0
Average Bed T (°C)	831	832	826	839	816	833	740	711
Average TC04 - TC05 (°C)	876	875	851	864	853	872	823	790
Average TC06 - TC07 (°C)	838	857	818	855	819	859	803	818
Gas Yield (Nm^3 dnf/kg daf)	1.19	1.23	0.87	0.88	0.88	0.99	0.61	1.01
LHV product gas (MJ/Nm^3 dry)	5.50	5.47	4.20	4.59	4.25	4.90	5.12	6.44
H_20 (vol%)	25.6	24.4	29.8	18.0	27.8	28.2	31.8	47.4
H_2 (vol% dnf)	28.7(± 0.2)	24.8(± 0.1)	29.4(± 0.7)	33.4(± 0.7)	28.8(± 0.6)	32.7(± 0.4)	39.4(± 1.2)	44.2(± 1.4)
CO (vol% dnf)	30.9(± 0.3)	31.4(± 0.2)	28.8(± 1.1)	27.6(± 0.6)	29.1(± 0.8)	27.8(± 0.7)	23.6(± 1.8)	20.3(± 1.6)
CH_4 (vol% dnf)	9.9(± 0.1)	10.5(± 0.1)	9.5(± 0.4)	9.3(± 0.2)	9.7(± 0.4)	9.3(± 0.3)	10.9(± 0.4)	9.3(± 0.6)
CO_2 (vol% dnf)	30.5(±0.3)	33.3(± 0.3)	32.3(± 1.1)	29.7(± 1)	32.4(± 0.8)	30.2(± 0.8)	26.1(± 1)	26.2(± 0.3)
N_2 (vol% db)	52.3(± 1)	51.6(± 0.5)	62.4(± 1.4)	59.9(± 1.4)	62.0(± 1.3)	56.9(± 1.3)	58.5(± 1.4)	45.8(± 3.5)
CGE (%)	74.7	75.4	52.3	54.2	53.3	60.9	40.4	65.1
OE (%)	41.3	43.1	27.9	28.8	28.4	32.8	19.3	31.0
Tars in total gas (g/Nm^3)	21.2	21.8	8.3	12.8	10.5	17.6	22.8	45.0
Benzene (g/kg daf)	1.34	1.40	0.37	0.96	0.52	1.13	1.62	2.90
Heterocyclic (g/kg daf)	5.1E-03	2.9E-03	3.1E-04	5.2E-03	3.6E-04	3.7E-03	7.1E-04	5.3E-02
Light Aromatic (g/kg daf)	1.2E-01	9.3E-02	1.2E-01	1.0E-01	1.5E-01	1.0E-01	3.6E-01	6.5E-01
Light PAH (g/kg daf)	7.1E-01	7.3E-01	3.7E-01	2.7E-01	4.1E-01	6.1E-01	1.0E+00	2.3E+00
Heavy PAH (g/kg daf)	7.1E-02	8.3E-02	3.1E-02	1.4E-02	3.4E-02	2.7E-02	1.4E-02	9.0E-02

Effect of steam/air gasification duration in the IHBFBSR on various process parameters and product yields (experiments 9–12).

Index (#)	9		10		11		12	
Set Point	SP1	SP2	SP1	SP2	SP1	SP2	SP1	SP2
Bed Material	F046	F046	F046	F046	F054	F054	F054	F054
Biomass	ExR	ExR	ExR	ExR	ExR	ExR	ExR	ExR
λ(−)	0.04	0.04	0.04	0.04	0.04	0.04	0.04	0.04
STBR (−)	1.2	1.2	1.2	1.2	1.2	1.2	1.2	1.2
Sec. air (kg/h)	8	8	4	4	4	4	8	8
Average Bed T (°C)	733	704	702	710	717	715	727	722
Average TC04 - TC05 (°C)	828	770	792	757	794	745	808	754
Average TC06 - TC07 (°C)	860	857	839	857	828	848	859	856
Gas Yield (Nm^3 dnf/kg daf)	0.86	0.87	0.77	0.92	0.69	0.94	0.85	1.05
LHV product gas (MJ/Nm^3 dry)	4.26	3.96	4.79	4.86	4.65	5.00	4.16	4.32
H_20 (vol%)	25.3	23.8	29.1	25.7	30.4	23.7	29.0	23.9
H_2 (vol% dnf)	31.6(± 0.7)	38.2(± 0.7)	34.7(± 1.1)	44.2(± 0.5)	31.9(± 0.9)	43.2(± 0.6)	31.4(± 0.9)	41.3(± 0.4)
CO (vol% dnf)	29.6(± 1.4)	22.5(± 0.4)	25.5(± 1.2)	19.3(± 0.3)	29.8(± 1.5)	20.3(± 0.8)	30.2(± 1.4)	21.6(± 0.4)
CH_4 (vol% dnf)	10.1(± 0.4)	7.9(± 0.2)	11.4(± 0.4)	7.6(± 0.3)	11.9(± 0.3)	8.1(± 0.5)	9.6(± 0.4)	6.5(± 0.4)
CO_2 (vol% dnf)	28.7(± 1)	31.4(± 0.8)	28.4(± 0.6)	28.9(± 0.3)	26.3(± 0.8)	28.5(± 1.1)	28.8(± 0.8)	30.6(± 0.5)
N_2 (vol% db)	63.9(± 1.3)	63.5(± 6)	60.7(± 0.8)	56.3(± 1.5)	63.1(± 1.1)	55.7(± 1.7)	64.2(± 1.4)	59.1(± 1.2)
CGE (%)	54.6	51.1	50.6	55.3	47.2	57.4	53.1	59.9
OE (%)	27.0	26.2	24.1	26.3	22.5	27.4	25.9	30.0
Tars in total gas (g/Nm^3)	13.3	3.9	7.7	4.9	8.1	5.1	3.0	1.9
Benzene (g/kg daf)	0.84	0.29	0.43	0.36	0.47	0.43	0.22	0.18
Heterocyclic (g/kg daf)	4.1E-04	1.1E-03	5.9E-03	4.8E-03	6.9E-03	1.5E-03	4.6E-03	1.3E-04
Light Aromatic (g/kg daf)	1.9E-01	1.5E-02	4.9E-02	3.4E-02	4.1E-02	2.5E-02	1.1E-02	4.3E-03
Light PAH (g/kg daf)	5.8E-01	1.8E-01	5.1E-01	2.5E-01	4.8E-01	2.2E-01	1.3E-01	6.4E-02
Heavy PAH (g/kg daf)	2.6E-02	1.6E-02	1.8E-02	6.5E-03	2.3E-02	1.1E-02	4.4E-03	1.1E-03

bed for SP2 vs SP1, which promotes tar decomposition and permanent gases formation, potentially explains the observed behaviour. The increase of the gaseous yield appears to be more significant for LT experiments (average increase of 0.21 versus 0.05 Nm^3 dnf/kg daf), further substantiating this conclusion (Table 5). Additionally, apart from HT experiment 5 with PG as a feedstock, the influence of extended duration of the experiment was beneficial for the H_2 yield, which increased by 4 vol% on average for HT and 8 vol% for LT experiments, between SP1 and SP2. Therefore, H_2 production is positively associated with tar catalytic conversion in the accumulated char bed [70]. In the previous section, it was argued that the effect of secondary air injection on tar reduction and therefore H_2 production for LT experiments, is more effective than the higher bed temperatures of the HT experiments in that regard. This is showcased again here, along with the also aforementioned positive impact of secondary air injection on the H_2 yield. Contrary to H_2, the CO and CH_4 were lower for SP2. The effect of longer steam/air gasification duration was again more significant for the LT experiments regarding these two gases. For CO, its yields decreased by 7 vol% for LT experiments versus less than 1 vol% for HT on average, between SP1 and SP2. CH_4 yields decreased by 3 vol% for HT experiments versus less than 1 vol% for LT experiments between SP1 and SP2. Finally, the CO_2 yields presented a small increase (1 vol% on average) for the LT experiments.

4.4.2. Tar and benzene composition

For HT experiments (5, 6 and 7), the tar content in the product gas increased between SP1 and SP2. The increase was marginal (3 wt%) for the PG experiment, but quite substantial for the two HT / ExR experiments (53 wt% and 68 wt%, respectively). For the PG experiment, the marginal difference can be attributed to the minor temperature

differences between the set points. In the two ExR experiments a higher λ was employed for SP1, which can explain the higher tar production presented for SP2. Furthermore, char accumulation does not take place on a large extent in HT experiments, preventing tar catalytic cracking at such levels as for the LT experiments. Regarding individual tar compounds, for both those experiments benzene production more than doubled, while phenol yield increased by one order of magnitude, between SP1 and SP2. Contrary to that however, the tar yield increased between SP1 and SP2 for the LT experiment 8. Most of the tar species content doubled, as well as benzene's, between those two sampling points. Phenol concentration in particular, increased by a factor of 74. The fact that char accumulation under these experimental conditions is not enough for tar catalytic cracking to an appreciable extent is showcased by phenol behaviour in particular. In general, char promotes the decomposition of oxygenated compounds even at temperatures lower than the ones achieved in this case [71]. Despite the fact that lower temperatures were achieved for the LT experiments and thus the effect of thermal cracking of phenol was less than for the HT ones, the reduction of its yield between SP1 and SP2, further supports the argument. Additionally, heavy PAH production also increased significantly from SP1 to SP2, with the yields of benzo(*k*)fluoranthene, benzo(*a*)pyrene and benzo(*b*)fluoranthene, increasing by ~400, 200 and 250 times, respectively. The yields of those three species combined, contribute to ~1 wt% of the overall tar and benzene yield, therefore the differences between the set points are subject to a thin margin of sampling error. However, heavy PAH species are of a high importance, since even in low concentrations they can influence the tar dew point greatly [72]. This behaviour of experiment 8, can be attributed to the different temperature between the two set points. Namely, the bed and TC04 – TC05 temperature decreased by approximately 30 °C for both regions. The increase of temperature in the TC06 – TC07 region from 803 °C to 818 °C, was not enough for sufficient thermal cracking of the produced tars. Therefore, despite the presence of the accumulated char bed, the temperature of the freeboard and the method of air supply are very critical for tar removal during steam/air gasification in the IHBFBSR. This remark can be well established through the differences between SP1 and SP2 for LT experiments 9, 10, 11 and 12. Starting with the overall tar content of the product gas, its reduction was significant in all four experiments from SP1 to SP2 (Table 5). The light and heavy PAH yield decreased by approximately 56 wt% on average, while the effect on benzene was similar but less pronounced. The catalytic effect of the char accumulated in the IHBFBSR is showcased by the decrease by ~52 wt% on average, of the naphthalene yield for these LT experiments, from SP1 to SP2. In general, naphthalene is stable up to temperatures around 900 °C in a steam/CO_2 environment [73]. Therefore, the reduction of its yield between SP1 and SP2 for the LT experiments with secondary air as shown here, can be partly attributed to the presence of char in the bed. The effect of the use of char as a catalyst for the conversion of tar and in particular naphthalene, which is also here the most abundant tar specie formed, has been well described by El-Rub in [74]. According to this work, tar is adsorbed on active sites of the surface of char particles and undergoes catalytic conversion through two parallel pathways. The first one involves steam and dry gasification reactions for the formation of CO and H_2, catalysed by the char's mineral content. The second path is centred around tar decomposition for the formation of free radicals, which polymerize and form coke deposits on the char surface. According to Burhenne et al. [75], the presence of CO_2 leads to further activation of the char bed which improves benzene removal, although the effect of steam is more pronounced, especially in the context of the hereby presented IHBFBSR experiments. In general, it can be argued that despite that char accumulates continuously in the IHBFBSR bed, the product yields do stabilize to the hereby presented values (SP2), signalling that tar conversion peaks, but also does not fall below that point. As it has been argued by El-Rub [74], char activity does not decrease with time since its micropores grow to *meso* and macro pores, which are more effective on tar removal and the accessible mineral content increases with the conversion of its carbon content. Lastly, for the IHBFBSR, the char keeps accumulating in the bed as long as gasification continues. Thus it can be argued that the efficiency of the tar conversion process is capped from the process conditions (temperature, λ, method of air supply, bed material, etc.) rather than the char catalyst's activity, as it has also been shown in [76]. High temperatures in particular have been shown to favour tar decomposition over a char bed [77,78]. Furthermore, as it has been suggested in [79] for the combined use of char and oxidation for tar removal, for high O_2 concentrations, char BET surface area can decrease significantly, due to partial oxidation. The fact that air can be added above the accumulated char bed in the IHBFBSR can address this problem and provide more flexibility on the amount of oxidizing agent added. Overall, the detailed analysis of the properties of the char derived from the IHBFBSR experiments (e.g. BET analysis, SEM, XRD, etc.), despite being relevant, was outside the scope of the present study. The corresponding investigation will be presented by the authors in a future study.

Table 6
Process conditions, working principles, performances and main gas compositions of Milena (ECN part of TNO), FICFB (TU Vienna), SilvaGas, Battelle (USA) and HPR (TU Munich) allothermal gasifiers.

	MILENA [80–85]	FICFB [86–88]	SilvaGas [89,90]	HPR [21,28,91]	IHBFBSR [this study]
Reformer					
Type	CFB	BFB	CFB	FBR	BFB
Agent	Steam	Steam	Steam	Steam	Steam/air
Pressure	atm	atm	atm	2–10 bar	atm
Temperature (°C)	>700	850–900	800–1000	700–800	700–850
Combustor					
Type	BFB	CFB	CFB	FBR	Burner
Performance					
Carbon Conversion (%)	100	100	100	86	82–95
Cold Gas Efficiency (%)	80*	80**	70	70	51–84
Product gas composition (vol% dnf)					
H_2	20	34	19	45	36
CO	50	24	54	21	26
CO_2	13	30	10	24	30
CH_4	17	12	17	10	9
Ratios (–)					
H_2:CO	0.4	1.4	0.4	2.2	1.5
H_2:CO_2	1.6	1.1	1.9	1.9	1.2
CO:CO_2	4.0	0.8	5.3	0.9	0.9
CH_4:H_2	0.8	0.4	0.9	0.2	0.3

* Taking into account gas cleaning.
** Total efficiency Güssing plant.

4.5. Comparison of IHBFBSR with other allothermal gasification concepts

As it can be seen in Table 6, the overall performance of the IHBFBSR during these commissioning experiments, compares well with other established allothermal gasification systems, some of which were already discussed in the introduction section. This is mainly in terms of cold gas efficiency and gas composition. The carbon conversion of the IHBFBSR was lower compared to the other systems with the exception of the HPR, which is also the most similar concept to the one employed here. Furthermore, it presented higher H_2:CO ratios among the non-pressurized systems (thus excluding the HPR). Overall, the hereby presented allothermal gasification concept is still in an early developmental stage and no extensive process optimization has yet been performed. Therefore, further comparison with these established technologies would not be meaningful. However, these initial results and comparison

provide an important benchmark for future investigation and showcase the potential of the IHBFBSR concept.

5. Conclusions

In this work, the results from the commissioning experiments on the novel IHBFBSR were presented, along with a description of its operational characteristics for a wide range of experimental conditions. During the investigation, the importance of the char accumulating in the bed area for the overall process was highlighted, since it appeared to promote H_2 production and in-situ tar destruction especially for smaller bed material particle sizes. Furthermore, it was found that the injection of moderate amounts of air in the freeboard can improve tar reduction and to a lesser extent CCE without negatively impacting H_2 production, even when compared to the introduction of larger amounts as a fluidization agent. Overall, the present study offers a thorough presentation of the IHBFBSR attributes for a variety of process conditions, allowing its use as a benchmark for similar systems and future works.

The product gas composition and CGE obtained from the IHBFBSR is favourably compared to some similar allothermal gasification systems, while carbon conversion can still be improved. Although the presence of the accumulated char bed can have a positive effect on syngas composition in terms of quality and tar content, a compromise between this effect and the increase of carbon conversion must be found. Additionally, the in-depth investigation of process hydrodynamics and heat/mass transfer characteristics through e.g. computational fluid dynamics, can provide important insights as to the improvement of the IHBFBSR's operation. The overall efficiency of the system can also be improved through for example, the increase of the burners output and efficiency and better insulation. Especially in the freeboard, with the addition of secondary air, lower temperatures and/or burner outputs could suffice for the required levels of tar removal. In general, the investigation of more tar reduction methods either in-situ (e.g. tar reducing bed material like olivine) or ex-situ (gas cleaning) should also be performed. Conclusively, despite the initial results being quite promising in terms of the scale-up potential of the IHBFBSR, significant reactor development work remains to be done.

Declaration of Competing Interest

The authors declare that they have no known competing financial interests or personal relationships that could have appeared to influence the work reported in this paper.

Acknowledgements

The authors would like to thank the Dutch company Petrogas Gas – Systems for co-financing the project. Funding was also received from European Union's Horizon 2020 Research and Innovation Programme under grant agreement number 731101 (BRISK II).

Appendix A

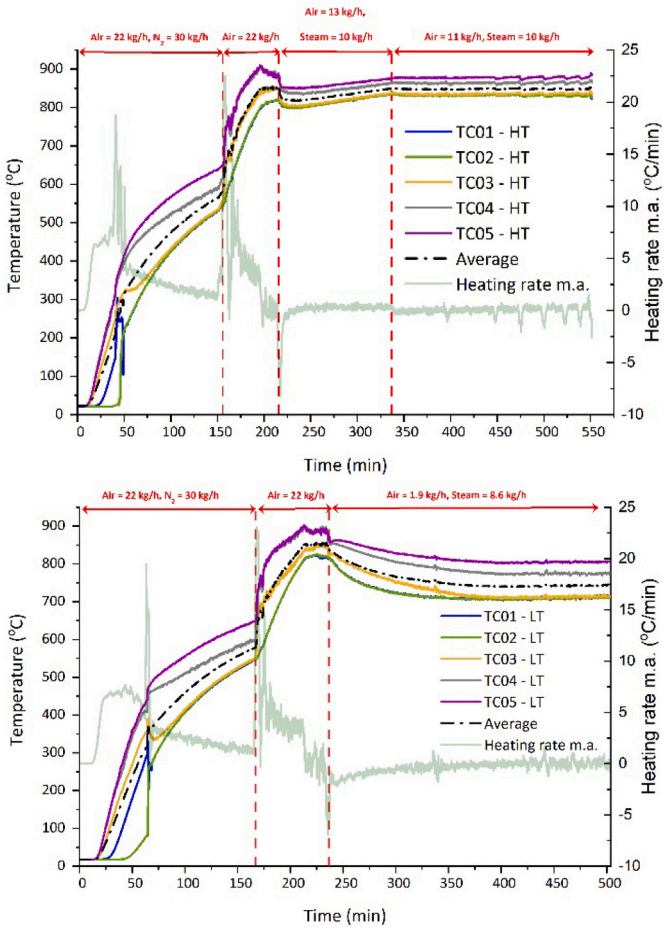

Fig. A.1. Temperature profile of the IHBFBSR bed and initial freeboard zone (thermocouples: TC01-TC05) for a high temperature (HT, top) and a low temperature (LT, bottom) steam gasification experiment with ExR as a feedstock and corundum F046 as bed material. The heating rate moving average refers to the average bed

temperature heating rate with a period of 20.

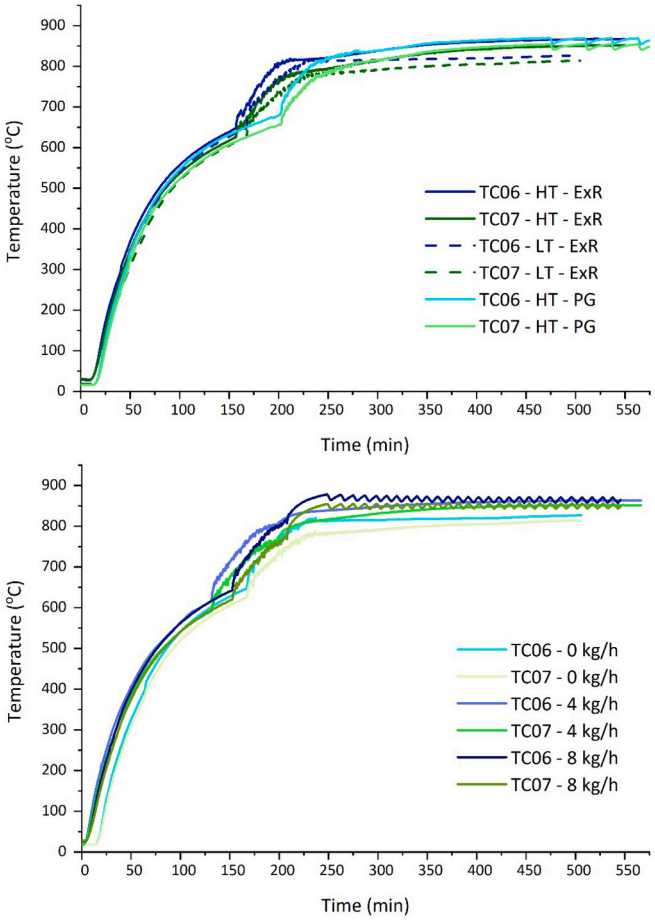

Fig. A.2. Temperature profile of the freeboard zone of the IHBFBSR (TC06 – TC07) for a high (HT) and a low (LT) temperature steam gasification experiment with ExR and a HT with PG as a feedstock and corundum F046 as bed material (top) with STBR = 1.2. On the bottom, again the temperature profile of the freeboard zone of the IHBFBSR (TC06 – TC07) for LT experiments in which various amounts of secondary air were injected (0, 4 and 8 kg/h) with ExR as a feedstock and corundum F046 as bed material under $\lambda = 0.04$ and STBR = 1.2. The LT experiment on the top is the same as the 0 kg/h one on the bottom.

References

[1] S. Wang, G. Dai, H. Yang, Z. Luo, Lignocellulosic biomass pyrolysis mechanism: a state-of-the-art review, Prog. Energy Combust. Sci. 62 (2017) 33–86.
[2] P. Basu, Biomass Gasification and Pyrolysis Practical Design and Theory, Elsevier Inc., 2010.
[3] V.S. Sikarwar, M. Zhao, P. Clough, J. Yao, X. Zhong, M.Z. Memon, N. Shah, E. J. Anthony, P.S. Fennell, An overview of advances in biomass gasification, Energy Environ. Sci. 9 (2016) 2939–2977.
[4] V. Belgiorno, G. De Feo, C. Della Rocca, R.M.A. Napoli, Energy from gasification of solid wastes, Waste Manag. 23 (2003) 1–15.
[5] A. Gómez-Barea, M. Suárez-Almeida, A. Ghoniem, Analysis of fluidized bed gasification of biomass assisted by solar-heated particles, Biomass Conv. Biorefinery 11 (2021) 143–158.
[6] O. Levenspiel, What will come after petroleum? Ind. Eng. Chem. Res. 44 (2005) 5073–5078.
[7] J. Karl, T. Pröll, Steam gasification of biomass in dual fluidized bed gasifiers: a review, Renew. Sust. Energ. Rev. 98 (2018) 64–78.
[8] J.C. Schmid, F. Benedikt, J. Fuchs, A.M. Mauerhofer, S. Müller, H. Hofbauer, Syngas for biorefineries from thermochemical gasification of lignocellulosic fuels and residues—5 years' experience with an advanced dual fluidized bed gasifier design, Biomass Conv. Biorefinery (2019) 1–38.
[9] K. Fürsatz, J. Fuchs, F. Benedikt, M. Kuba, H. Hofbauer, Effect of biomass fuel ash and bed material on the product gas composition in DFB steam gasification, Energy 219 (2021) 119650.
[10] A.M. Mauerhofer, F. Benedikt, J.C. Schmid, J. Fuchs, S. Müller, H. Hofbauer, Influence of different bed material mixtures on dual fluidized bed steam gasification, Energy 157 (2018) 957–968.
[11] H. Thunman, M. Seemann, T. Berdugo Vilches, J. Maric, D. Pallares, H. Ström, G. Berndes, P. Knutsson, A. Larsson, C. Breitholtz, O. Santos, Advanced biofuel production via gasification – lessons learned from 200 man-years of research activity with Chalmers' research gasifier and the GoBiGas demonstration plant, Energy Sci. Eng. 6 (2018) 6–34.
[12] Gussing Renewable Energy. http://www.gussingrenewable.com/ (20/05/2021).
[13] Project Gaya. https://www.projetgaya.com/ (20/05/2021).
[14] M. Martín-Gamboa, D. Iribarren, A. Susmozas, J. Dufour, Delving into sensible measures to enhance the environmental performance of biohydrogen: a quantitative approach based on process simulation, life cycle assessment and data envelopment analysis, Bioresour. Technol. 214 (2016) 376–385.
[15] E.T. Liakakou, B.J. Vreugdenhil, N. Cerone, F. Zimbardi, F. Pinto, R. André, P. Marques, R. Mata, F. Girio, Gasification of lignin-rich residues for the production of biofuels via syngas fermentation: Comparison of gasification technologies, Fuel 251 (2019) 580–592.
[16] C.M. van der Meijden, H.J. Veringa, L.P.L.M. Rabou, The production of synthetic natural gas (SNG): a comparison of three wood gasification systems for energy balance and overall efficiency, Biomass Bioenergy 34 (2010) 302–311.
[17] E.T. Liakakou, A. Infantes, A. Neumann, B.J. Vreugdenhil, Connecting gasification with syngas fermentation: Comparison of the performance of lignin and beech wood, Fuel 290 (2021) 120054.
[18] A. Larsson, M. Kuba, T. Berdugo Vilches, M. Seemann, H. Hofbauer, H. Thunman, Steam gasification of biomass – typical gas quality and operational strategies derived from industrial-scale plants, Fuel Process. Technol. 212 (2021) 106609.
[19] N. Hanchate, S. Ramani, C.S. Mathpati, V.H. Dalvi, Biomass gasification using dual fluidized bed gasification systems: a review, J. Clean. Prod. 280 (2021) 123148.
[20] H. Jüntgen, K.H. Van Heek, Gasification of coal with steam using heat from HTRs, Nucl. Eng. Des. 34 (1975) 59–63.
[21] J. Karl, Biomass heat pipe reformer—design and performance of an indirectly heated steam gasifier, Biomass Conv. Biorefinery 4 (2014) 1–14.
[22] Y. Inaba, M. Fumizawa, M. Tonogouchi, Y. Takenaka, Coal gasification system using nuclear heat for ammonia production, Appl. Energy 67 (2000) 395–406.
[23] H. Kubiak, H.-J. Schröter, A. Sulimma, K.-H. van Heek, Application of K2CO3 catalysts in the coal gasification process using nuclear heat, Fuel 62 (1983) 242–245.

[24] J.M. Lee, Y.J. Kim, S.D. Kim, Catalytic coal gasification in an internally circulating fluidized bed reactor with draft tube, Appl. Therm. Eng. 18 (1998) 1013–1024.
[25] M. Naqvi, J. Yan, E. Dahlquist, Black liquor gasification integrated in pulp and paper mills: a critical review, Bioresour. Technol. 101 (2010) 8001–8015.
[26] R.H. Williams, E.D. Larson, R.E. Katofsky, J. Chen, Methanol and hydrogen from biomass for transportation, Energy Sustain. Dev. 1 (1995) 18–34.
[27] P. Treiber. https://www.evt.tf.fau.eu/research/schwerpunkte/verbrennung-vergasung-von-biomasse/heatpipe-reformer/ (26/01/2021).
[28] J.M. Leimert, P. Treiber, J. Karl, The Heatpipe Reformer with optimized combustor design for enhanced cold gas efficiency, Fuel Process. Technol. 141 (2016) 68–73.
[29] G. Gallmetzer, P. Ackermann, A. Schweiger, T. Kienberger, T. Gröbl, H. Walter, M. Zankl, M. Kröner, The agnion Heatpipe-Reformer—operating experiences and evaluation of fuel conversion and syngas composition, Biomass Conv. Biorefinery 2 (2012) 207–215.
[30] S. Karellas, J. Karl, E. Kakaras, An innovative biomass gasification process and its coupling with microturbine and fuel cell systems, Energy 33 (2008) 284–291.
[31] J.P.A. Neeft, H.A.M. Knoef, G.J. Buffinga, U.A. Zielke, K.A. Sjöström, C.A. Brage, P. A. Hasler, P.A.A. Smell, M. Suomalainen, M.A.A. Dorrington, C.A. Greil, Guideline for sampling and analysis of tars and particles in biomass producer gases, in: Progress in Thermochemical Biomass Conversion, 2001, pp. 162–175.
[32] A. Sluiter, B. Hames, D. Hyman, C. Payne, R. Ruiz, C. Scarlata, J. Sluiter, D. Templeton, J. Wolfe, Biomass and Total Dissolved Solids in Liquid Process Samples, in: National Renewable Energy Laboratory (NREL/TP-510-42621), 2008.
[33] A. Sluiter, B. Hames, R. Ruiz, C. Scarlata, J. Sluiter, D. Templeton, Determination of Ash in Biomass, in: National Renewable Energy Laboratory (NREL/TP-510-42622), 2008.
[34] O. Levenspiel, Chemical Reaction Engineering, 3d ed., 1998.
[35] M. Siedlecki, On the Gasification of Biomass in a Steam-Oxygen Blown CFB Gasifier with the Focus on Gas Quality Upgrading: Technology Background, Experiments and Mathematical Modeling, in, Delft University of Technology, 2011.
[36] M. Di Marcello, G.A. Tsalidis, G. Spinelli, W. de Jong, J.H.A. Kiel, Pilot scale steam-oxygen CFB gasification of commercial torrefied wood pellets. The effect of torrefaction on the gasification performance, Biomass Bioenergy 105 (2017) 411–420.
[37] M. Siedlecki, W. De Jong, A.H.M. Verkooijen, Fluidized bed gasification as a mature and reliable technology for the production of bio-syngas and applied in the production of liquid transportation fuels—A review, Energies 4 (2011) 389–434.
[38] Y. Kalinci, A. Hepbasli, I. Dincer, Biomass-based hydrogen production: a review and analysis, Int. J. Hydrog. Energy 34 (2009) 8799–8817.
[39] H. de Lasa, E. Salaices, J. Mazumder, R. Lucky, Catalytic Steam Gasification of Biomass: Catalysts, Thermodynamics and Kinetics, Chem. Rev. 111 (2011) 5404–5433.
[40] A. Kumar, K. Eskridge, D.D. Jones, M.A. Hanna, Steam–air fluidized bed gasification of distillers grains: Effects of steam to biomass ratio, equivalence ratio and gasification temperature, Bioresour. Technol. 100 (2009) 2062–2068.
[41] S. Kern, C. Pfeifer, H. Hofbauer, Gasification of lignite in a dual fluidized bed gasifier — Influence of bed material particle size and the amount of steam, Fuel Process. Technol. 111 (2013) 1–13.
[42] D. Geldart, The effect of particle size and size distribution on the behaviour of gas-fluidised beds, Powder Technol. 6 (1972) 201–215.
[43] S. Turn, C. Kinoshita, Z. Zhang, D. Ishimura, J. Zhou, An experimental investigation of hydrogen production from biomass gasification, Int. J. Hydrog. Energy 23 (1998) 641–648.
[44] N.B. Klinghoffer, M.J. Castaldi, A. Nzihou, Influence of char composition and inorganics on catalytic activity of char from biomass gasification, Fuel 157 (2015) 37–47.
[45] S. Hosokai, K. Kumabe, M. Ohshita, K. Norinaga, C.-Z. Li, J.-i. Hayashi, Mechanism of decomposition of aromatics over charcoal and necessary condition for maintaining its activity, Fuel 87 (2008) 2914–2922.
[46] Z. Abu El-Rub, E.A. Bramer, G. Brem, Review of catalysts for tar elimination in biomass gasification processes, Ind. Eng. Chem. Res. 43 (2004) 6911–6919.
[47] L. Devi, K.J. Ptasinski, F.J.J.G. Janssen, A review of the primary measures for tar elimination in biomass gasification processes, Biomass Bioenergy 24 (2003) 125–140.
[48] X. Meng, W. de Jong, N. Fu, A.H.M. Verkooijen, Biomass gasification in a 100 kWth steam-oxygen blown circulating fluidized bed gasifier: Effects of operational conditions on product gas distribution and tar formation, Biomass Bioenergy 35 (2011) 2910–2924.
[49] L. Devi, K.J. Ptasinski, F.J.J.G. Janssen, S.V.B. van Paasen, P.C.A. Bergman, J.H. A. Kiel, Catalytic decomposition of biomass tars: use of dolomite and untreated olivine, Renew. Energy 30 (2005) 565–587.
[50] A. Jess, Mechanisms and kinetics of thermal reactions of aromatic hydrocarbons from pyrolysis of solid fuels, Fuel 75 (1996) 1441–1448.
[51] Z. Zhang, S. Pang, Experimental investigation of tar formation and producer gas composition in biomass steam gasification in a 100 kW dual fluidised bed gasifier, Renew. Energy 132 (2019) 416–424.
[52] B.J. Vreugdenhil, R.W.R. Zwart, Tar formation in pyrolysis and gasification, in: ECN-E–08-087, ECN - Energy Research Centre of the Netherlands, 2009.
[53] M. Mayerhofer, P. Mitsakis, X. Meng, W. de Jong, H. Spliethoff, M. Gaderer, Influence of pressure, temperature and steam on tar and gas in allothermal fluidized bed gasification, Fuel 99 (2012) 204–209.
[54] D. Fuentes-Cano, A. Gómez-Barea, S. Nilsson, P. Ollero, The influence of temperature and steam on the yields of tar and light hydrocarbon compounds during devolatilization of dried sewage sludge in a fluidized bed, Fuel 108 (2013) 341–350.
[55] P.A. Simell, E.K. Hirvensalo, V.T. Smolander, A.O.I. Krause, Steam reforming of gasification gas tar over dolomite with benzene as a model compound, Ind. Eng. Chem. Res. 38 (1999) 1250–1257.
[56] Y.H. Qin, J. Feng, W.Y. Li, Formation of tar and its characterization during air–steam gasification of sawdust in a fluidized bed reactor, Fuel 89 (2010) 1344–1347.
[57] P.M. Lv, Z.H. Xiong, J. Chang, C.Z. Wu, Y. Chen, J.X. Zhu, An experimental study on biomass air–steam gasification in a fluidized bed, Bioresour. Technol. 95 (2004) 95–101.
[58] C.M. Kinoshita, Y. Wang, J. Zhou, Tar formation under different biomass gasification conditions, J. Anal. Appl. Pyrolysis 29 (1994) 169–181.
[59] J.J. Hernández, R. Ballesteros, G. Aranda, Characterisation of tars from biomass gasification: effect of the operating conditions, Energy 50 (2013) 333–342.
[60] P. Morf, P. Hasler, T. Nussbaumer, Mechanisms and kinetics of homogeneous secondary reactions of tar from continuous pyrolysis of wood chips, Fuel 81 (2002) 843–853.
[61] T.A. Milne, R.J. Evans, N. Abatzoglou, Biomass Gasifier "Tars": Their Nature, Formation, and Conversion, in: National Renewable Energy Laboratory (NREL) (NREL/TP-570-25357), 1998.
[62] J. Gil, J. Corella, M.A.P. Aznar, M.A. Caballero, Biomass gasification in atmospheric and bubbling fluidized bed: effect of the type of gasifying agent on the product distribution, Biomass Bioenergy 17 (1999) 389–403.
[63] Y.G. Pan, X. Roca, E. Velo, L. Puigjaner, Removal of tar by secondary air in fluidised bed gasification of residual biomass and coal, Fuel 78 (1999) 1703–1709.
[64] T. Robinson, B. Bronson, P. Gogolek, P. Mehrani, Comparison of the air-blown bubbling fluidized bed gasification of wood and wood–PET pellets, Fuel 178 (2016) 263–271.
[65] Y. Cao, Y. Wang, J.T. Riley, W.-P. Pan, A novel biomass air gasification process for producing tar-free higher heating value fuel gas, Fuel Process. Technol. 87 (2006) 343–353.
[66] A. Gómez-Barea, B. Leckner, A. Villanueva Perales, S. Nilsson, D. Fuentes Cano, Improving the performance of fluidized bed biomass/waste gasifiers for distributed electricity: a new three-stage gasification system, Appl. Therm. Eng. 50 (2013) 1453–1462.
[67] M. Campoy, A. Gómez-Barea, D. Fuentes-Cano, P. Ollero, Tar Reduction by primary measures in an Autothermal Air-Blown Fluidized Bed Biomass Gasifier, Ind. Eng. Chem. Res. 49 (2010) 11294–11301.
[68] Y. Zhang, S. Kajitani, M. Ashizawa, Y. Oki, Tar destruction and coke formation during rapid pyrolysis and gasification of biomass in a drop-tube furnace, Fuel 89 (2010) 302–309.
[69] G.A. Tsalidis, C. Tsekos, K. Anastasakis, W. de Jong, The impact of dry torrefaction on the fast pyrolysis behavior of ash wood and commercial Dutch mixed wood in a pyroprobe, Fuel Process. Technol. 177 (2018) 255–265.
[70] G. Ravenni, O.H. Elhami, J. Ahrenfeldt, U.B. Henriksen, Y. Neubauer, Adsorption and decomposition of tar model compounds over the surface of gasification char and active carbon within the temperature range 250–800 °C, Appl. Energy 241 (2019) 139–151.
[71] Q. Sun, S. Yu, F. Wang, J. Wang, Decomposition and gasification of pyrolysis volatiles from pine wood through a bed of hot char, Fuel 90 (2011) 1041–1048.
[72] C. Li, K. Suzuki, Tar property, analysis, reforming mechanism and model for biomass gasification—an overview, Renew. Sust. Energ. Rev. 13 (2009) 594–604.
[73] Z. Abu El-Rub, E.A. Bramer, G. Brem, Experimental comparison of biomass chars with other catalysts for tar reduction, Fuel 87 (2008) 2243–2252.
[74] Z. Abu El-Rub, Biomass Char as an In-Situ Catalyst for Tar Removal in Gasification Systems, in, University of Twente, Enschede, 2008.
[75] L. Burhenne, T. Aicher, Benzene removal over a fixed bed of wood char: the effect of pyrolysis temperature and activation with CO2 on the char reactivity, Fuel Process. Technol. 127 (2014) 140–148.
[76] P. Gilbert, C. Ryu, V. Sharifi, J. Swithenbank, Tar reduction in pyrolysis vapours from biomass over a hot char bed, Bioresour. Technol. 100 (2009) 6045–6051.
[77] J. Park, Y. Lee, C. Ryu, Reduction of primary tar vapor from biomass by hot char particles in fixed bed gasification, Biomass Bioenergy 90 (2016) 114–121.
[78] F. Dabai, N. Paterson, M. Millan, P. Fennell, R. Kandiyoti, Tar formation and destruction in a fixed-bed reactor simulating downdraft gasification: equipment development and characterization of tar-cracking products, Energy Fuel 24 (2010) 4560–4570.
[79] S. Zhao, Y. Luo, Y. Zhang, Y. Long, Experimental investigation of the synergy effect of partial oxidation and bio-char on biomass tar reduction, J. Anal. Appl. Pyrolysis 112 (2015) 262–269.
[80] B. Drift, C. Meijden, M. Boerrigter, MILENA gasification technology for high efficient SNG production from biomass, in: ECN-RX-05-183, ECN - Energy Research Centre of the Netherlands, 2005.
[81] C. Meijden, B. Drift, Waste wood fueled gasification demonstration project, in: ECN-M–11-066, ECN - Energy Research Centre of the Netherlands, 2011.
[82] C. Meijden, B. Vreugdenhil, B. Drift, Experimental results from the allothermal biomass gasifier Milena, in: 15th European Biomass Conference & Exhibition, Berlin, Germany, 2008.
[83] C. Meijden, L.P.L.M. Rabou, B. Boven, M. Overwijk, Production of bio methane from wood using the MILENA gasification technology, in: ECN-M–15-044, ECN - Energy Research Centre of the Netherlands, 2014.
[84] C. Meijden, Development of the MILENA gasification technology for the production of bio-SNG, in: Chemical Engineering and Chemistry, Technische Universiteit Eindhoven, Eindhoven, 2010.
[85] C. Meijden, H. Veringa, B. Drift, B. Vreugdenhil, The 800 kWth allothermal biomass gasifier MILENA, in: 16th European Biomass Conference & Exhibition, Valencia, Spain, 2008.

[86] H. Hofbauer, G. Veronik, T. Fleck, R. Rauch, H. Mackinger, E. Fercher, The FICFB — Gasification Process, in: A.V. Bridgwater, D.G.B. Boocock (Eds.), Developments in Thermochemical Biomass Conversion: Volume 1 / Volume 2, Springer Netherlands, Dordrecht, 1997, pp. 1016–1025.
[87] R. Rauch, H. Hofbauer, K. Bosch, I. Siefert, C. Aichernig, H. Tremmel, Steam gasification of biomass at CHP plant in guessing - status of the demonstration plant, in: Second World Conference and Technology Exhibition, 2004, pp. 1–4.
[88] T. Pröll, R. Rauch, C. Aichernig, H. Hofbauer, Fluidized bed steam gasification of solid biomass - performance characteristics of an 8 MWth combined heat and power plant, Int. J. Chem. React. Eng. 5 (2007).
[89] M.A. Paisley, R. Overend, Verification of the performance of future energy resources' silvagas biomass gasifier - operating experience in the vermont gasifier, in: Pittsburgh Coal Conference, 2002.
[90] S. Babu, Biomass Gasification for Hydrogen Production–Process Description and Research Needs, Gas Technology Institute, Des Plaines, Illinois, USA, 2005.
[91] J.M. Leimert, P. Treiber, M. Neubert, A. Sieber, J. Karl, Performance of a 100 kW Heatpipe Reformer Operating on Lignite, Energy Fuel 31 (2017) 4939–4950.